THE UNIVERSITY OF MANITOBA

LIBRARY

AUTHOR DE JONG, Mark Sybe

TITLE THE DESIGN OF AN H- AND D- POLARIZED ION SOURCE AND RESONANT DEPOLARIZATION OF POLARIZED H- IONS IN A CYCLOTRON

THESIS Ph.D., 1981

I, the undersigned, agree to refrain from producing, or reproducing, the above-named work, or any part thereof, in any material form, without the written consent of the author:

A. ROONAS

THE DESIGN OF AN H^- AND D^- POLARIZED ION SOURCE AND RESONANT DEPOLARIZATION OF POLARIZED H^- IONS IN A CYCLOTRON

BY

MARK SYBE DE JONG

A thesis
presented to the University of Manitoba
in partial fulfillment of the
requirements for the degree of
Doctor of Philosophy
in
Department of Physics

Winnipeg, Manitoba, 1981

THE UNIVERSITY OF MANITOBA

FACULTY OF GRADUATE STUDIES

The undersigned certify that they have read, and recommend to the Faculty of Graduate Studies for acceptance, a Ph.D. thesis entitled: The Design of an H^- and D^- Polarized Ion Source and Resonant Depolarization of Polarized H^- Ions in a Cyclotron.

submitted by Mark DeJong

in partial fulfilment of the requirements for the Ph.D. degree.

Advisor

Advisor

Dr. Michael Craddock
External Examiner
Department of Physics
Univ. of British Columbia
Vancouver, B.C.

Date of oral examination: 1st Sept. 1981

The student has satisfactorily completed and passed the Ph.D. oral examination.

Chairman of Ph.D. Oral*

(*The signature of the Chairman does not necessarily signify that the Chairman has read the complete thesis.)

THE DESIGN OF AN H^- AND D^- POLARIZED ION SOURCE AND RESONANT DEPOLARIZATION OF POLARIZED H^- IONS IN A CYCLOTRON

BY

MARK SYBE DE JONG

A thesis submitted to the Faculty of Graduate Studies of the University of Manitoba in partial fulfillment of the requirements of the degree of

DOCTOR OF PHILOSOPHY

ABSTRACT

A polarized H^- and D^- ion source of the nuclear spin filter type has been constructed for the University of Manitoba cyclotron. This source has been tested and performs reliably with an average output beam current of 100 nA of either H^- or D^- ions for injection into the cyclotron. The nuclear scattering experiments, $^4He(\vec{p},p)^4He$ and $^4He(\vec{d},d)^4He$, were performed to measure the polarization of the beams after acceleration in the cyclotron. The polarization measurements of the D^- beam were in good agreement with the quench ratio estimates. However, the polarization measurements of the accelerated H^- beam were near zero, very dependent upon the operating conditions of the cyclotron, and in disagreement with the quench ratio estimates.

This reduced polarization of the H^- beam has been explained by resonant depolarization of the beam during acceleration in the cyclotron. An intrinsic depolarizing resonance of the form $\gamma G = -4 + \nu_z$ occurs at 9.0 MeV. Analytic estimates and detailed numerical calculations of the polarization loss predict a net polarization near zero, in good agreement with the H^- polarization measurements. These calculations represent the first close examination of serious resonant depolarization in an isochronous cyclotron.

TABLE OF CONTENTS

ACKNOWLEDGMENTS

I would like to thank my supervisor, Dr. Saewoong Oh, for his guidance, patience, and advice while I was working on this project. I have profitted greatly from our many lengthy discussions. I would also like to thank Dr. J. S. C. McKee who first suggested this project and his continued support since then.

Both the Physics Department's electronics shop and machine shop have been of immense help.

The assistance of all of the cyclotron's technical support staff, in particular that of John Bruckshaw and Robert Pogson, is also gratefully acknowledged.

Special thanks are also due to Jim Birchall and all the graduate students who worked many long hours helping with the polarization measurements.

I would also like to thank the cyclotron development group at TRIUMF who provided the original versions of the programs POLICY, CYCLOP, and GOBLIN, and especially Dr. M. Craddock for his comments and advice on the resonant depolarization.

Funding for this project was provided, in part, by N.S.E.R.C.

Finally, I must express heartfelt thanks to my wife, Mary, for her tolerance and patience over the past few years.

LIST OF FIGURES

PAGE

FIGURE

CHAPTER 1

INTRODUCTION

Over the past twenty years interest in the nuclear spin dependence of reactions in nuclear and particle physics has steadily increased. The measurement of polarization observables contributes essential data necessary for the successful interpretation of many experiments. Analyzing power and spin-spin correlation measurements are needed to remove many ambiguities which arise in phase shift analyses. Experiments determining the scattering asymmetry in various nuclear reactions have aided the spin and parity assignments of many excited states of nuclei. Even possible violations of some of the fundamental symmetries of nature, conservation of parity, charge symmetry, time reversal invariance, or isospin invariance, are now being studied with very precise polarization experiments. More detail of many of these experiments is given in the proceedings of the five Polarization Symposia (see Polarization Symposia 1961, 1966, 1971, 1976, 1981).

With an eye on this trend, the decision to develop a polarized beam facility at the University of Manitoba Cyclotron Laboratory was made in 1974. The

University of Manitoba cyclotron (Standing et al., 1962) is a sector-focussed isochronous cyclotron designed for the acceleration of H^- ions, with the first beam accelerated in 1964. The acceleration of negative ions provides an efficient method of extraction through the stripping of the two electrons. The result is an external proton beam with an energy variable from 20 to 50 MeV. D^- ions may also be accelerated providing a deuteron beam with an energy from 10 to 25 MeV, but this requires halving the radio frequency of the accelerating electric field, and extensive re-trimming of the magnetic field. Consequently no experiments with the deuteron beam had been performed until 1980.

In preparation for a polarized ion source, an axial injection system permitting operation of the cyclotron with larger external ion sources was completed in 1975 (see Batten et al., 1976). The phase space acceptance of this injection system was quite small because of the compactness of the central region of the cyclotron. This constraint, and the fact that only H^- and D^- ions could be accelerated were the main determining factors in the choice of the type of polarized ion source.

At that time there were two main types of sources for polarized hydrogen isotopes, atomic beam sources and Lamb shift sources (see, for instance, Glavish, 1974

for a review of polarized ion sources). Atomic beam sources capable of producing from 10 μA to 30 μA of polarized H^+ or D^+ ions, or 0.3 μA of H^- or D^- ions were available. The total emittance area was typically 50 mm mrad $MeV^{1/2}$ with energy spreads less than ± 100 eV. The Lamb shift sources could provide from 0.1 to 0.3 μA of polarized H^- or D^- ions but with a much lower energy spread of about ±10 eV (McKibben et al., 1974) and a smaller emittance. Since there was not much difference in the beam intensities for negative ions, a Lamb shift type source design was chosen because of its better beam quality.

The rapid aquisition of experience in developing and operating a Lamb shift source was obtained by using the small Sona type polarized H^- ion source developed at the University of Alberta as a prototype for the TRIUMF cyclotron (McIlwain et al., 1978). Although some polarized beam was accelerated and a polarization of $p_z = 0.26 \pm 0.03$ was measured, successful operation of the source was hampered by very poor transmission through the cyclotron resulting in only 3 pA of beam on target, and by a lack of reproducibility of the polarization measurements.

While operating experience with this first source was being gathered another Lamb shift source of the nuclear spin filter type was being designed. Polarized

H^- ions from this source were first accelerated in January 1979. The transmission through the cyclotron with this new source was much better, usually about 10% which was the same as for unpolarized H^- ions. However, the difficulties in obtaining reproducible polarization measurements persisted.

By January 1980, after much experimental effort over the preceeding year, it was concluded that the irreproducibility was probably due to resonant depolarization of the polarized H^- ions during acceleration in the cyclotron. Estimates of the severity of the resonant depolarization of polarized D^- ions accelerated in the University of Manitoba cyclotron indicated that no significant loss of polarization should occur. The decision to attempt acceleration of polarized D^- ions was made in March 1980 based on these estimates. By May 1980 a beam of 12 nA of polarized deuterons was extracted from the cyclotron at 12.6 MeV. Measurements of the polarization showed no loss of polarization, within statistical error, and an experiment measuring A_y and A_{yy} in $^4He(\vec{d},d)^4He$ scattering was performed. This achievement represented several firsts: (1) The first experiment with deuterons at the University of Manitoba, (2) The first polarized D^- ions accelerated in a cyclotron, and (3) The first use of a nuclear spin filter type ion source on a cyclotron.

When analyzing the severity of the resonant depolarization of H^- ions, several shortcomings were found in the earlier studies on this subject. The significant difference between accelerating polarized H^- ions compared to polarized H^+ ions was not clearly appreciated. Several inconsistencies had to be resolved, and several extensions of the analyses had to be performed to permit careful comparison between the analytic estimates, the detailed numerical simulations, and the experimental results. This is believed to be the first such analysis for severe resonant depolarization in an isochronous cyclotron.

This thesis will report on the development and testing of the University of Manitoba polarized ion source. Chapter 2 will review the theoretical background of the Lamb shift nuclear spin filter type ion source. Chapter 3 will cover the details of the U of M source and will discuss several of its limitations. Chapter 4 will discuss the techniques used to measure the polarization and the results for H^- and D^- ions. Chapter 5 will review the origins of resonant depolarization and will give an analysis of its occurrence for polarized H^- ions in the U of M cyclotron. Finally Chapter 6 will summarize the present status of the polarized ion facility and will point to several areas where possible improvements may be made.

CHAPTER 2

POLARIZED HYDROGEN AND DEUTERIUM BEAMS

2.1 Nuclear Polarization

A beam of particles with nuclear spin I is said to be polarized if the probability of finding a particle in a substate $|I, m_I\rangle$ is not $(2I + 1)^{-1}$, i.e. if the particles do not randomly populate all the possible substates. In the case of polarized H^- ions $I = 1/2$, and there are only two possible substates. If the ion's quantization axis is taken to be the z-axis, and n_+ and n_- are the probabilities that an ion is in the $m_I = 1/2$ or $m_I = -1/2$ substates then the polarization p_z of the beam is defined to be:

$$p_z = n_+ - n_- \tag{1}$$

Hence a beam of H^- ions all in the $m_I = 1/2$ or $m_I = -1/2$ substates has a nuclear polarization of $p_z = 1$ or $p_z = -1$ respectively.

The situation with polarized D^- ions is somewhat more complicated. Here two types of polarizations are defined, although they are not completely independent. Let n_+', n_0', and n_-' be the probabilities of an ion in the beam being in the $m_I = 1$, $m_I = 0$, or $m_I = -1$

substates with respects to quantization along the z-axis. Then the vector polarization is again defined to be:

$$p_z = n_+' - n_-' \tag{2}$$

and the tensor polarization is defined to be:

$$p_{zz} = 1 - 3n_o' \tag{3}$$

Refer to Darden, (1971) for more detail on the various types of polarization and their nomenclature.

2.2 Atomic Structure of Metastable Hydrogen and Deuterium Atoms

All Lamb shift polarized ion sources for hydrogen isotopes are based upon the production of a beam of hydrogen atoms in the metastable 2S state with nuclear polarization. To explain how a nuclear spin filter produces such a beam from an unpolarized beam of metastable atoms it is necessary to briefly review the fine and hyperfine structure of the atomic levels with principal quantum number n = 2 in hydrogen and deuterium atoms (see Lamb, 1952; Bethe and Salpeter, 1957; or Ohlsen and McKibben, 1967). These levels lie about 10.20 eV above the ground state and consist of the $2S_{1/2}$, $2P_{1/2}$, and $2P_{3/2}$ levels. In a region of space free of electric and magnetic fields, the $2S_{1/2}$ state lies 1058 MHz above the $2P_{1/2}$ state (this is known as the Lamb shift) and the $2P_{3/2} - 2P_{1/2}$

separation is about 10.968 GHz. The $2P_{1/2}$ and $2P_{3/2}$ states have lifetimes of approximately 1.6 ns before decaying to the $1S_{1/2}$ ground state via an electric dipole transition. However, a $2S_{1/2}$ to $1S_{1/2}$ transition is strongly forbidden and a $2S_{1/2}$ to $2P_{1/2}$ transition is very weak due to the small energy difference between these states, so that the unperturbed $2S_{1/2}$ state is metastable with a lifetime of about 0.14 s.

If a relatively weak magnetic field is applied, fine structure splitting occurs due to the interaction of the magnetic field with the electron's magnetic moment and the electron's orbital motion. This is known as the Zeeman effect and is shown in figure 1. The interaction Hamiltonian which describes this splitting is given by:

$$\begin{aligned} H &= - \vec{\mu} \cdot \vec{B} \\ &= \mu_b (L_z + g_s S_z) B \end{aligned} \tag{4}$$

where the z-axis is taken to be parallel to the magnetic field $\vec{B}$, $\mu_b = \hbar e/(2m_e)$ is the Bohr magneton, g_s is the g-value of the electron's spin, and L_z and S_z are respectively the orbital and spin angular momentum z-axis projection operators.

The energy level shifts from the unperturbed states are then given in terms of $\vec{L}$, $\vec{S}$ and $\vec{J} = \vec{L} + \vec{S}$ by:

$$\Delta E = \mu_b g_L B m \tag{5}$$

Figure 1. Fine structure of the hydrogen atom with principal quantum number n = 2.

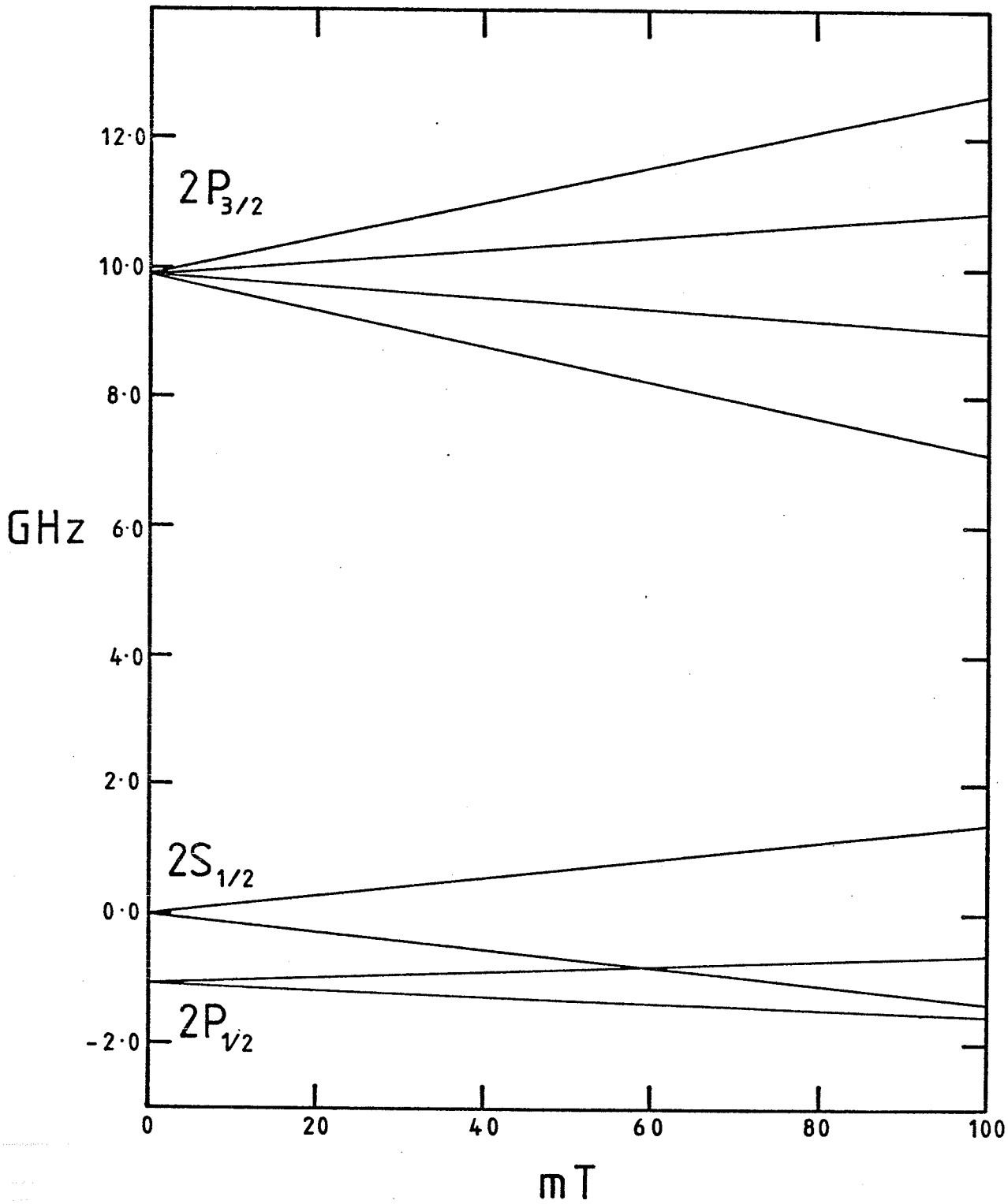
12·0
10·0
8·0
6·0
4·0
2·0
0·0
-2·0
GHz
2P3/2
2S1/2
2P1/2
0
20
40
60
80
100
mT

for the states with a z-axis angular momentum projection of $m = -J, -J + 1, \ldots, J$, and for g_L, the Landé g-factor, given by:

$$g_L = \frac{(J(J + 1) - S(S + 1) + L(L + 1))}{2J(J + 1)} + g_s \frac{(J(J + 1) + S(S + 1) - L(L + 1))}{2J(J + 1)} \tag{6}$$

It is important to notice that the $2S_{1/2}$ ($m_J = -1/2$) and the $2P_{1/2}$ ($m_J = 1/2$) states become degenerate at fields of about 57.5 mT since the nuclear spin filter takes advantage of this fact.

If the energy levels in magnetic fields of this strength are examined more closely, each level is actually split into two levels for hydrogen and three levels for deuterium. This hyperfine splitting is due to the interaction of the nuclear magnetic moment with the electron's magnetic moment, as well as with the external magnetic field. The complete Hamiltonian is now given by:

$$H = \alpha \vec{I} \cdot \vec{J} + g_L \mu_b \vec{J} \cdot \vec{B} + g_I \mu_n \vec{I} \cdot \vec{B} \tag{7}$$

where α determines the hyperfine splitting due to the coupling of the nuclear magnetic moment to the electron's total angular momentum, μ_n is the nuclear magneton and g_I is the nuclear g-factor.

Approximate solutions for the eigenstates and

eigenvalues of equation (7) separate naturally into two forms, depending upon whether $\alpha >> g_L \mu_b B$, the weak field limit, or $\alpha << g_L \mu_b B$, the strong field or Back-Goudsmit limit. In the weak field limit the appropriate basis states are $|F, m_F>$, i.e. those of total angular momentum $\vec{F} = \vec{I} + \vec{J}$, which are the exact eigenstates for zero external magnetic field. As the strength of an applied magnetic field increases, $\vec{F}$ no longer remains a good quantum number since $\vec{J}$ and $\vec{I}$ begin to couple more strongly to the field than to each other. Once in the strong field region, $\vec{J}$ and $\vec{I}$ are essentially decoupled and the appropriate basis states are the tensor product of the $|J, m_J>$ and $|I, m_I>$ states. This latter representation is preferred for all field strengths when calculations are performed for the polarized sources. The reason is that only the nuclear spin state portion is of interest and this appears explicitly in the $|J, m_J>|I, m_I>$ representation.

Equation (7) can be diagonalized analytically in this basis set (see Ohlsen, 1970). Only those hyperfine states which lie in the $2S_{1/2}$, $m_J = 1/2$ level can be transmitted by the nuclear spin filter, so only these will be considered in detail. The eigenvalues or energies (expressed in frequency units) of these levels for the case of $J = 1/2$ and arbitrary I is given by the Breit-Rabi formula:

$$E = \frac{-\Delta W}{2(2I+1)} + g_I \mu_n B m \pm \left(\frac{\Delta W}{2}\right)\left(1 + \frac{4mx}{(2I+1)} + x^2\right)^{1/2} \qquad (8)$$

where ΔW is the field free hyperfine splitting,

$$m = m_I + m_J = m_I + \frac{1}{2} \qquad (9)$$

and

$$\begin{aligned} x &= (g_L \mu_b - g_I \mu_n) B/\Delta W \\ &= B/B_1 \end{aligned} \qquad (10)$$

which is a dimensionless quantity representing the strength of the applied field. For hydrogen in the $2S_{1/2}$ states, ΔW = 177.551 MHz or B_1 = 6.345 mT, and for deuterium in the $2S_{1/2}$ states, ΔW = 40.924 MHz or B_1 = 1.460 mT. The eigenstates of the two hyperfine levels in the $2S_{1/2}$, m_J = 1/2 level of hydrogen are then given by:

$$\begin{aligned} &\text{State 1.} \quad \left|\tfrac{1}{2}, \tfrac{1}{2}\right\rangle \left|\tfrac{1}{2}, \tfrac{1}{2}\right\rangle \\ &\text{State 2.} \quad \left(\frac{1+\delta}{2}\right)^{1/2} \left|\tfrac{1}{2}, \tfrac{1}{2}\right\rangle \left|\tfrac{1}{2}, -\tfrac{1}{2}\right\rangle \\ &\qquad + \left(\frac{1-\delta}{2}\right)^{1/2} \left|\tfrac{1}{2}, -\tfrac{1}{2}\right\rangle \left|\tfrac{1}{2}, \tfrac{1}{2}\right\rangle \end{aligned} \qquad (11)$$

where:

$$\delta = x/(1 + x^2)^{1/2}$$

Similarly, the eigenstates of the three hyperfine

levels in the $2S_{1/2}$, $m_J = 1/2$ level of deuterium are:

$$\text{State 1.} \quad |\tfrac{1}{2}, \tfrac{1}{2}\rangle |1, 1\rangle$$

$$\text{State 2.} \quad \left(\frac{1 + \delta_+}{2}\right)^{1/2} |\tfrac{1}{2}, \tfrac{1}{2}\rangle |1, 0\rangle + \left(\frac{1 - \delta_+}{2}\right)^{1/2} |\tfrac{1}{2}, -\tfrac{1}{2}\rangle |1, 1\rangle \qquad (12)$$

$$\text{State 3.} \quad \left(\frac{1 + \delta_-}{2}\right)^{1/2} |\tfrac{1}{2}, \tfrac{1}{2}\rangle |1, -1\rangle + \left(\frac{1 - \delta_-}{2}\right)^{1/2} |\tfrac{1}{2}, -\tfrac{1}{2}\rangle |1, 0\rangle$$

where:

$$\delta_+ = \frac{x + 1/3}{(1 + 2x/3 + x^2)^{1/2}}$$

and

$$\delta_- = \frac{x - 1/3}{(1 - 2x/3 + x^2)^{1/2}}$$

The dependence of the nuclear polarization on the external magnetic field can now be given from the definitions of vector and tensor polarization and the eigenstates given above. The vector polarization for hydrogen is:

$$\text{State 1.} \quad p_z = 1$$

$$\text{State 2.} \quad p_z = -\delta \qquad (13)$$

levels in the $2S_{1/2}$, $m_J = 1/2$ level of deuterium are:

$$\text{State 1.} \quad |\tfrac{1}{2}, \tfrac{1}{2}\rangle|1, 1\rangle$$

$$\text{State 2.} \quad \left(\frac{1 + \delta_+}{2}\right)^{1/2} |\tfrac{1}{2}, \tfrac{1}{2}\rangle|1, 0\rangle + \left(\frac{1 - \delta_+}{2}\right)^{1/2} |\tfrac{1}{2}, -\tfrac{1}{2}\rangle|1, 1\rangle \qquad (12)$$

$$\text{State 3.} \quad \left(\frac{1 + \delta_-}{2}\right)^{1/2} |\tfrac{1}{2}, \tfrac{1}{2}\rangle|1, -1\rangle + \left(\frac{1 - \delta_-}{2}\right)^{1/2} |\tfrac{1}{2}, -\tfrac{1}{2}\rangle|1, 0\rangle$$

where:

$$\delta_+ = \frac{x + 1/3}{(1 + 2x/3 + x^2)^{1/2}}$$

and

$$\delta_- = \frac{x - 1/3}{(1 - 2x/3 + x^2)^{1/2}}$$

The dependence of the nuclear polarization on the external magnetic field can now be given from the definitions of vector and tensor polarization and the eigenstates given above. The vector polarization for hydrogen is:

$$\text{State 1.} \quad p_z = 1$$

$$\text{State 2.} \quad p_z = -\delta \qquad (13)$$

The polarizations of the deuterium are:

$$\begin{aligned} &\text{State 1.} && p_z = 1 \\ & && p_{zz} = -1 \\ &\text{State 2.} && p_z = (1 - \delta_+)/2 \\ & && p_{zz} = -(1 + 3\delta_+)/2 \\ &\text{State 3.} && p_z = -(1 + \delta_-)/2 \\ & && p_{zz} = -(1 - 3\delta_-)/2 \end{aligned} \tag{14}$$

2.3 The Theory of Nuclear Spin Filter Operation

A consequence of the hyperfine splitting is that the magnetic field at which the $2S_{1/2}$, $m_J = -1/2$ and the $2P_{1/2}$, $m_J = 1/2$ levels become degenerate depends upon the nuclear spin state, as shown in figures 2 and 3. If the magnetic field is adjusted so that this degeneracy occurs for a particular nuclear spin state, m_I, then those atoms originally in the $2S_{1/2}$, $m_J = 1/2$ state with that particular nuclear spin state will be transmitted through the spin filter unaltered. However all other "unselected" 2S states will be mixed with the $2P_{1/2}$ states and then decay to the 1S ground state before emerging from the nuclear spin filter. Thus one specific hyperfine state in the magnetic field is "filtered" from all the possible hyperfine states.

The specific technique used to achieve this

Figure 2. Hyperfine structure of the $2S_{1/2}$, $m_J = \pm 1/2$ and the $2P_{1/2}$, $m_J = 1/2$ levels in hydrogen. The dashed line indicates the 1.608 GHz radio-frequency transition for state (1) selection.

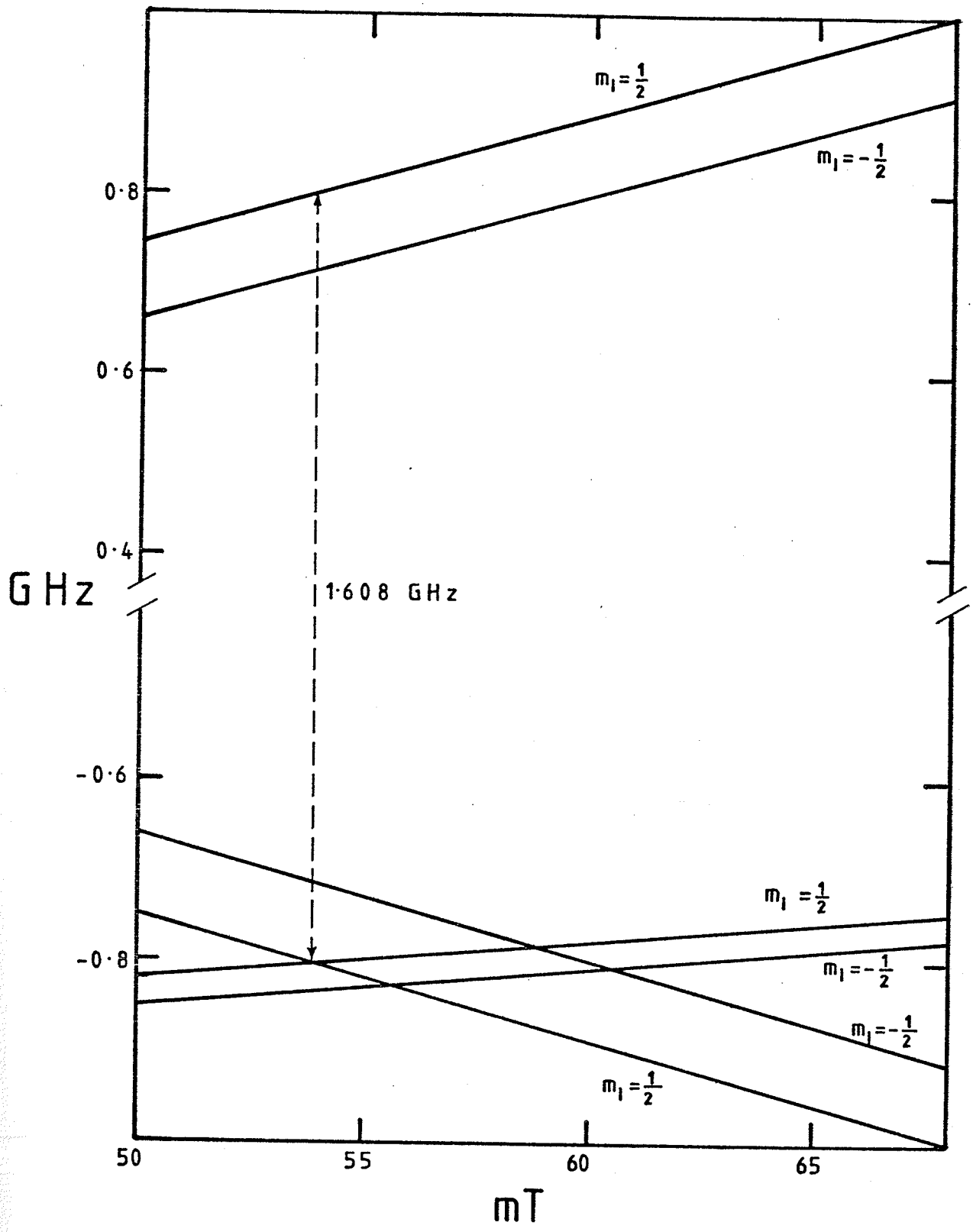
$m_I = \frac{1}{2}$
$m_I = -\frac{1}{2}$
0·8
0·6
0·4
GHz
1·608 GHz
-0·6
-0·8
$m_I = \frac{1}{2}$
$m_I = -\frac{1}{2}$
$m_I = -\frac{1}{2}$
$m_I = \frac{1}{2}$
50
55
60
65
mT

Figure 3. Hyperfine structure of the $2S_{1/2}$, $m_J = \pm 1/2$ and the $2P_{1/2}$, $m_J = 1/2$ levels in deuterium. The dashed lines 1, 2, and 3 indicate the 1.608 GHz transitions for state (1), state (2), and state(3) selection respectively.

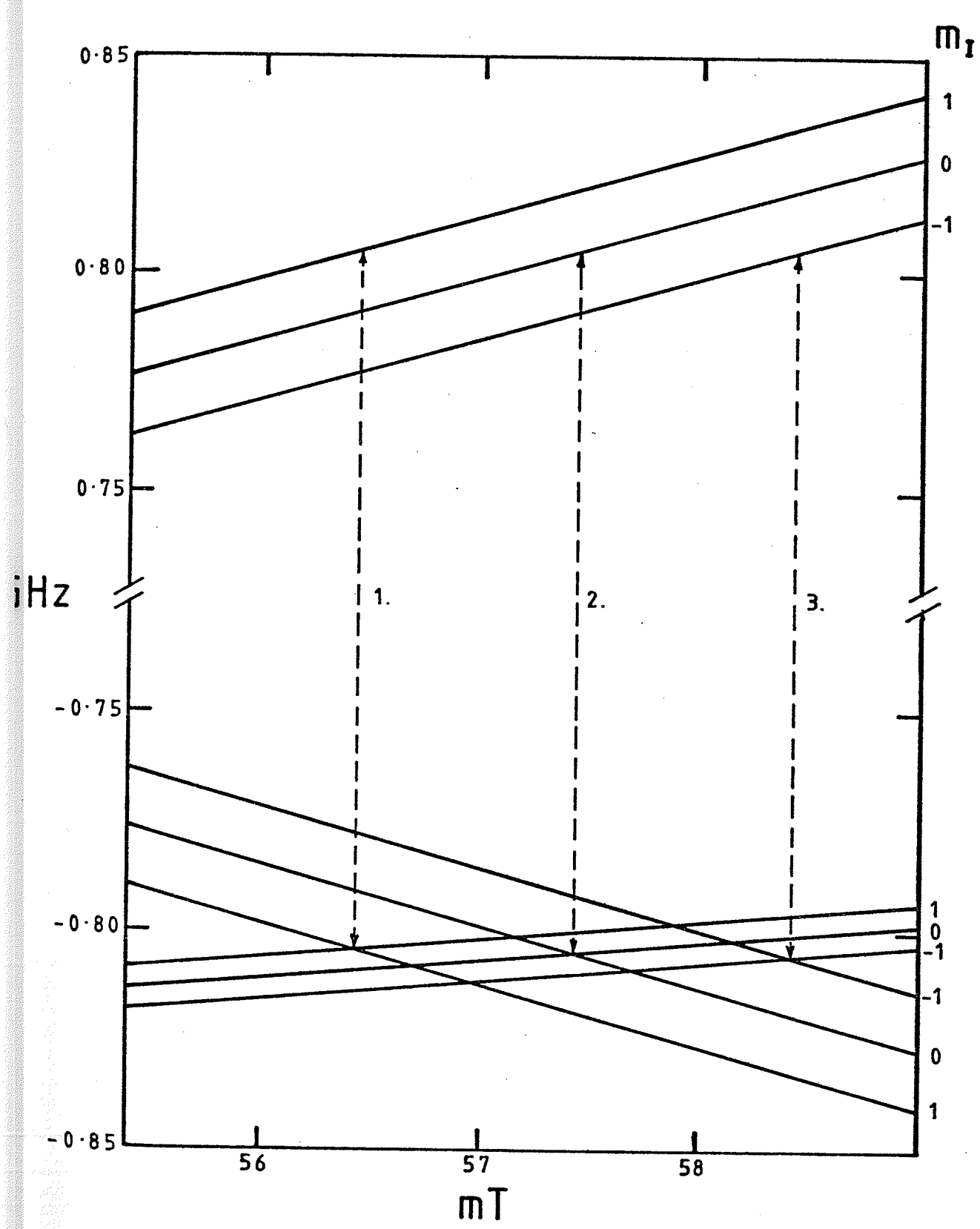
m_I
0·85
0·80
0·75
1
0
-1
iHz
1.
2.
3.
-0·75
-0·80
-0·85
1
0
-1
-1
0
1
56
57
58
mT

selection is based upon the "three level" interaction first described by Lamb (1952), and first applied to polarized ion sources by Ohlsen and McKibben (1967). The technique consists of a weak electric field of about 2.0 kV/m applied transversely to the beam of metastable hydrogen atoms, as well as an oscillating longitudinal electric field with a frequency of about 1.608 GHz and a similar peak electric field strength of about 2.0 kV/m. The static electric field mixes the $2S_{1/2}$, $m_J = -1/2$ and the $2P_{1/2}$, $m_J = 1/2$ states by the Stark effect. If only this field is applied, the lifetime of the $2S_{1/2}$, $m_J = -1/2$ states is reduced drastically compared to the $2S_{1/2}$, $m_J = 1/2$ states because of the rapid decay of the $2P_{1/2}$ states to the ground state. In the case of the oscillating electric field, the frequency corresponds to the $2P_{1/2}$, $m_J = 1/2$ to $2S_{1/2}$, $m_J = 1/2$ separation when the magnetic field is set such that the $2P_{1/2}$, $m_J = 1/2$ and the $2S_{1/2}$, $m_J = -1/2$ states are degenerate. Similarly, if only the oscillating field is applied then the lifetime of the $2S_{1/2}$, $m_J = 1/2$ state is drastically reduced because of the mixing of the $2S_{1/2}$, $m_J = 1/2$, and the $2P_{1/2}$, $m_J = 1/2$ states and the subsequent decay of the $2P_{1/2}$, $m_J = 1/2$ states.

However, if both fields are applied simultaneously, then the "three level" interaction occurs.

When the magnetic field is adjusted for the exact resonance, half of the atoms originally in the $2S_{1/2}$ state with the selected m_I remain in a $2S_{1/2}$ state with a long lifetime. This $2S_{1/2}$ state is a linear combination of the $m_J = +1/2$ and the $m_J = -1/2$ states. The other half is rapidly quenched to the 1S ground state. If both of the electric field strengths are then smoothly reduced to zero, then the unquenched atoms will all be in the $2S_{1/2}$, $m_J = 1/2$ state. The conditions for resonance depend very strongly on the magnetic field strength, a 0.5 mT deviation from resonance is sufficient to completely quench both $2S_{1/2}$ states. Since the hyperfine interaction causes the resonance magnetic field strength to depend on the nuclear spin state, a separation of the resonances of about 7.0 mT for hydrogen and about 1.0 mT for deuterium occurs. These splittings are larger than the width of the resonance, thus the atoms remaining in the $2S_{1/2}$ state after passage through the nuclear spin filter will be in one specific hyperfine state. If these atoms in the $2S_{1/2}$ state can then be selectively converted into positive or negative ions, then a beam of polarized protons or deuterons may be obtained.

CHAPTER 3

THE UNIVERSITY OF MANITOBA NUCLEAR SPIN FILTER POLARIZED ION SOURCE

3.1 Introduction to Polarized Ion Source Design

The general requirements for a polarized ion source of the nuclear spin filter type are now clear. A beam of hydrogen atoms in the 2S metastable state must be prepared. This beam is then passed through a nuclear spin filter, selecting atoms in a specific hyperfine state. These atoms, which remain in the 2S metastable state, are then converted into ions for subsequent acceleration, and their nuclear polarization is determined by the local magnetic field at the time of ionization.

3.2 The U of M Polarized Ion Source

In the U of M polarized ion source the beam of metastable hydrogen atoms is produced by extracting a beam of protons from a duoplasmatron ion source, and then passing the beam through a canal containing cesium vapor. At a proton energy of about 550 eV there is a maximum in the cross-section for the reaction:

$$H^+ + Cs \rightarrow H(2S) + Cs^+$$

which provides a convenient method for producing the metastable hydrogen atoms. After the hyperfine state selection in the nuclear spin filter, the beam of polarized metastable hydrogen atoms passes through a second charge exchange canal containing argon gas. Here the electron transfer reaction:

$$H(2S) + Ar \rightarrow H^- + Ar^+$$

occurs. The resulting beam of H^- ions is then accelerated to 11 keV for injection into the University of Manitoba cyclotron. If polarized D^- ions are preferred, then the first charge exchange on the cesium is performed at about 1.1 keV, and the injection energy is only 5.5 keV.

3.2.1 The Duoplasmatron

A positive ion duoplasmatron is used to provide the beam of H^+ or D^+ ions. The basic design of the one in the U of M source follows that in the Los Alamos van de Graaf polarized ion source (see Lawrence et al., 1969). In operation, a hydrogen arc of 5 to 10 A is struck between the filament and the anode. A strong axial magnetic field between the intermediate electrode and the anode compresses the arc radially creating a cylindrical plasma in this region. Some of the plasma leaks through a small aperture of 0.30 mm in the anode into the expansion cup region. Here the strong electric field

produced by the extractor accelerates all positive ions contained in the plasma in the expansion cup region. Usually, the extracted current consists of atomic H^+ ions as well as molecular H_2^+ and H_3^+ ions. The relative distribution of ion species as well as the total current can be adjusted by varying the arc current, the magnetic field strength, the hydrogen gas flow and the anode aperture size. A more complete description of the operation of duoplasmatron sources may be found in Lejeune (1974a, 1974b).

3.2.2 The Accel-decel Lens System

Figure 4 shows a cross-section of the plasma region of the duoplasmatron, the extractor, and the accel-decel lens system. The basic design problem here is to find a suitable method of extracting the hydrogen beam from the duoplasmatron and then focussing it through the cesium canal at an energy of only 550 eV. At this low energy, with the magnitude of current involved, the size of the beam rapidly expands due to the electrostatic repulsion between the ions within the beam. Such space-charge effects must be minimized.

First, although the desired beam energy at the cesium canal is 550 eV, this energy is far too low for the extraction of currents on the order of 1 mA from the duoplasmatron. For example, if the expansion cup and extractor region is approximated by a planar diode, then the maximum surface current density I_s (A/m^2) which can be extracted is given by (see Kirstein et al., 1967):

Figure 4. Duoplasmatron extraction region and the accel-decel lens system.

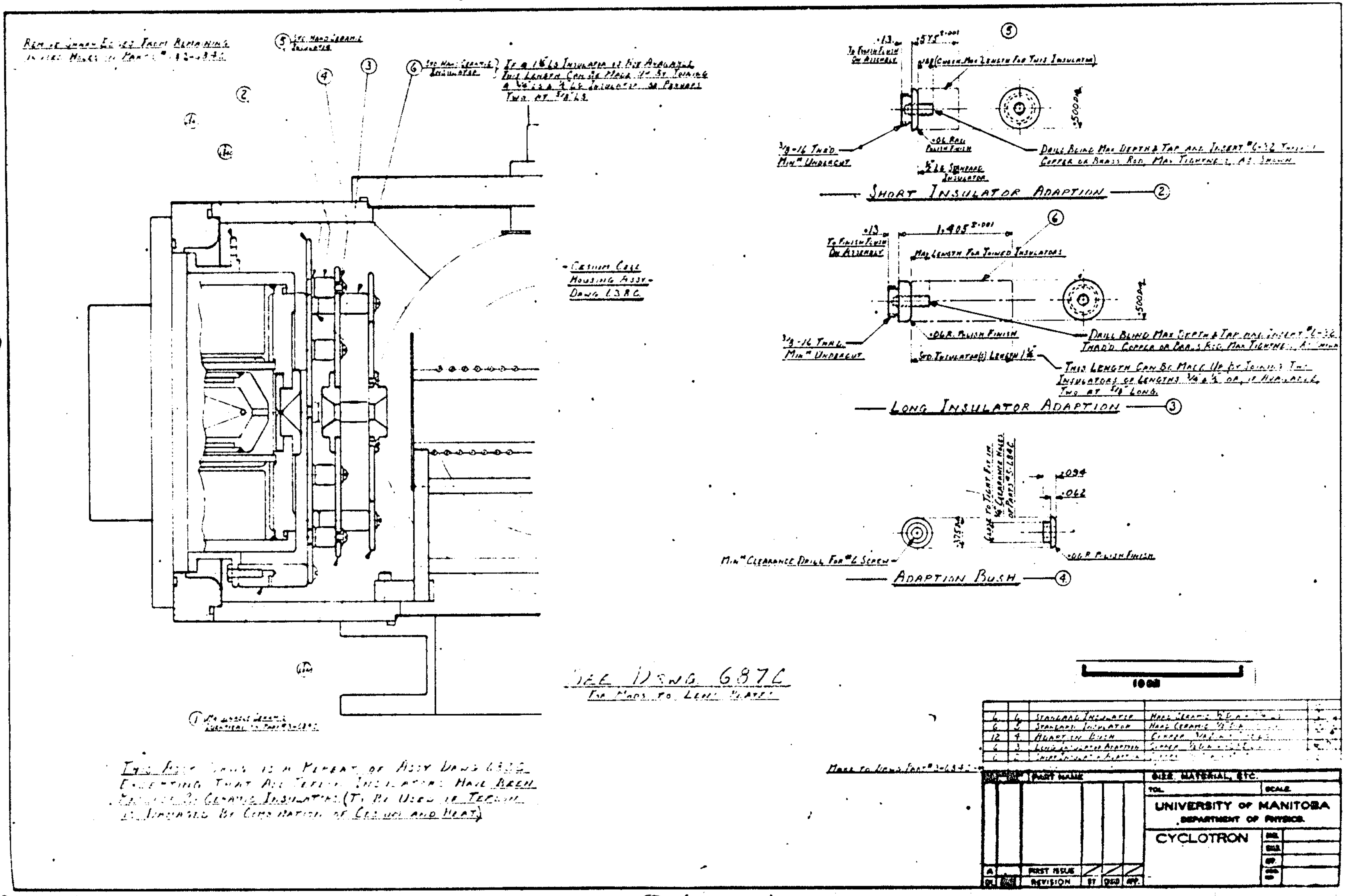
Short Insulator Adaption
Long Insulator Adaption
Adaption Bush
Cesium Case Housing Assy. Dwg. 638C
See Dwg 687C
3/8-16 Thr'd
Min. Undercut
.500 Dia
1.405
.094
.062
.375
1 Inch
UNIVERSITY OF MANITOBA
DEPARTMENT OF PHYSICS
CYCLOTRON
PART NAME
SIZE, MATERIAL, ETC.
FIRST ISSUE
REVISION

$$I_s = \frac{4}{9}\left(\frac{2q}{m}\right)^{1/2} \varepsilon_o V^{3/2} z^{-2} \qquad (1)$$

where V is the extractor voltage in volts, q is the charge of the ion in coulombs, m is the mass of the ion in kilograms, z is the plasma surface to extractor distance in meters and $\varepsilon_o = 8.854 \times 10^{-12}$ is the dielectric constant for free space. For a voltage of only 550 V and the typical separation of 13.5 mm, the maximum current density is 3.8 A/m^2. By examination of the expansion cup it is known that the plasma surface has a radius of approximately 3 mm which corresponds to a maximum current of only 0.1 mA. In practice, not only is the extracted current small but it is also strongly divergent after the extractor.

In order to extract considerably more current, as well as to provide better focussing of the beam, an accel-decel system is used (see Lawrence et al., 1969; or Green, 1976). Here the extraction voltage is increased to increase the total current extracted, and then the beam is decelerated to the desired energy. The strength of the focussing may be adjusted by varying both the extractor voltage and the separation of the extractor and the decel electrode. In the case of the U of M polarized ion source, it was found to be convenient to introduce a second high voltage electrode between the extractor and the decel electrode. Since the

position of each electrode is fixed, the voltage on this additional electrode gives an extra degree of freedom when focussing the beam through the cesium canal.

3.2.3 The Cesium Canal

Figure 5 shows a cross-section of the cesium canal. (Please note that figure 5 also shows some modifications to the accel-decel lens system, and in the region downstream from the cesium canal which have not been tested yet.) The oven can take up to 25 g of cesium metal but only 5 g is usually used. This is more than enough to operate for 2 weeks. The two heating coils can maintain the whole oven and canal assembly at a constant temperature which can be regulated to within $\pm$ 0.2° C. The normal operating temperature is about 100° C. The copper inserts into the main canal permit convenient variation of the effective canal diameter and length. Initially a large 25 mm diameter was used so that the canal would not limit the beam. However the excessive cesium loss rate made operation of the source unreliable since much of the lost cesium was deposited on the electrodes causing frequent high voltage breakdowns. Also the positive beam diameter was smaller than expected so the present 10 mm entrance diameter canal insert was made. The larger exit diameter allows for possible expansion of the beam size in the canal. The whole cesium canal assembly is in-

Figure 5. Cesium canal, modified accel-decel lens system and new post cesium canal deflection plates.

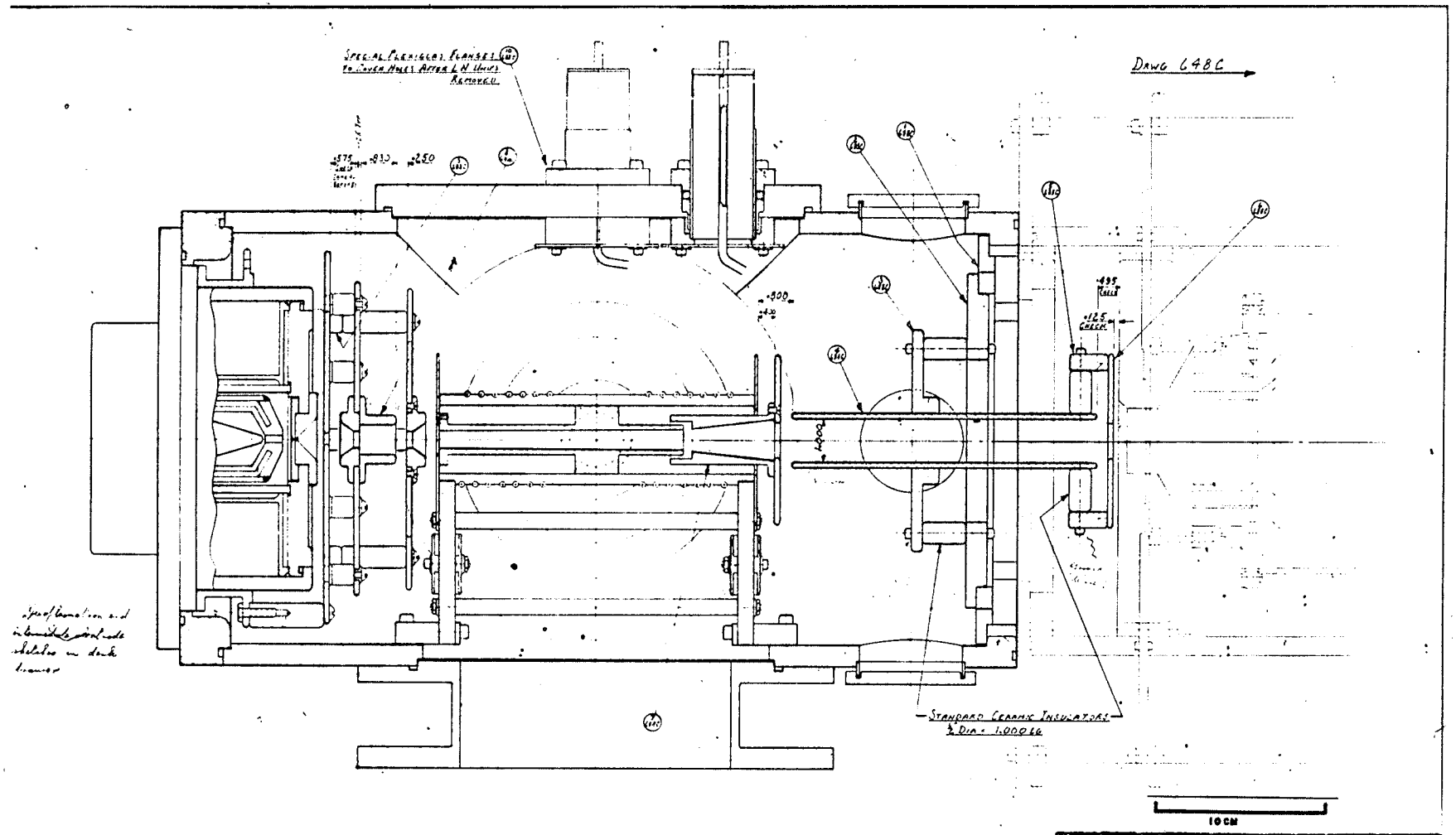

Specification and identification code details on data sheet

TO MEET SCALE A NUMBER OF TRIAL MODIFICATIONS ARE INCLUDED BE USED IN CONJUNCT ON WITH THE FIRST ASSEMBLY OF THIS SECTION 638C.
SEE ALSO ILLUSTRATION MOUNTED ON CESIUM CELL HOUSING DRWGS 638C & 641C

			PART NAME			SIZE, MATERIAL, ETC.	
						TOL.	SCALE
						UNIVERSITY OF MANITOBA	
						DEPARTMENT OF PHYSICS	
						CYCLOTRON	
A			FIRST ISSUE				
CH.	DATE		REVISION	BY	CHKD.	APP.	

sulated from the body of the ion source, and can be biased up to +150 V with respect to the body of the ion source. The biasing is used to help eliminate some background in the polarized beam by the velocity filter technique described in section 3.2.8. By inserting a plug into the oven which blocks all the incident beam, the whole cesium canal can also serve as a biased Faraday cup for diagnostic use.

3.2.4 Ion Optics Through the Cesium Canal

One of the strongest constraints on the maximum polarized current which can be produced from a Lamb shift source is the amount of positive current which can pass through the cesium canal to produce the metastable beam. As in the case with the extractor, the necessity of high beam currents at 550 eV results in significant space charge effects. The maximum current in amps, which can drift through a tube of radius a and length L is given by (see Kirstein et al., 1967):

$$I_m = 1.171\ \pi\ 8\varepsilon_o(2q/m)^{1/2}V^{3/2}(a/L)^2 \qquad (2)$$

where q is the charge of the ion, m is the mass of the ion and V is the electric potential of the tube. If a = 5 mm, the average radius of the cesium canal, then for protons at 550 eV the maximum possible current through the canal is 36 μA. In the case of deuterons at 1100 eV the maximum possible current is 72 μA.

However, unlike the situation in the extraction region, the beam energy cannot be varied here in order to reduce these space-charge effects. Fortunately the atomic collision processes which occur between the incident ions and the cesium vapor help to diminish the space-charge blow-up. In addition to the desired charge exchange reactions between the incident protons and the cesium atoms, ionization of the cesium atoms is also possible producing free electrons and positive cesium ions. The positive space-charge of the proton beam can trap these electrons while forcing the cesium ions out of the beam. The trapped electrons neutralize some of the space-charge of the proton beam and help to reduce its radial expansion. In practice, about 90% to 95% of the beam's space-charge can be neutralized permitting 10 to 20 times as much current to pass through the drift tube.

3.2.5 Atomic Processes in the Cesium Canal

As mentioned above, the most significant atomic process which occurs in the cesium canal is:

$$H^+ + Cs \rightarrow H(2S) + Cs^+$$

This reaction has a maximum cross-section of about 6×10^{-15} cm^2 at an energy of $\sim$ 500 eV (Pradel et al., 1974). However, for the production of an intense meta-

stable beam where various background contributions may be significant, all other important one step and two step processes should be examined. Thus the cross-sections for the following reactions are also important:

$$(1) \qquad H^+ + Cs \rightarrow H(1S) + Cs^+$$

The production of ground state hydrogen atoms forms a large neutral background. Most of these atoms are actually formed by the production of H(2P) atoms with a cross-section of 3×10^{-15} cm^2 (Pradel et al., 1974). But the lifetime of the 2P states is short so virtually all of these atoms have decayed to the ground state before leaving the cesium canal.

$$(2) \qquad H(2S) + Cs \rightarrow H(1S) + Cs$$

This collisional quenching of the metastable beam is the most significant loss mechanism of the H(2S) atoms, with a cross-section of 5×10^{-15} cm^2 (Pradel et al., 1974).

$$(3) \qquad H(2S) + Cs \rightarrow H^- + Cs^+$$
$$H(1S) + Cs \rightarrow H^- + Cs^+$$

These are the second steps in possible two step processes which form unpolarized H^- ions. These

must be removed from the polarized H^- ions formed later. The cross-sections for these processes have been estimated by Pradel et al. (1974) to be an order of magnitude smaller than the collisional quenching process described previously.

There exists an optimum cesium thickness of $\sim 1.2 \times 10^{14}$ atoms/cm^2 where approximately 0.30 of the original proton current is converted into metastable atoms. The same cross-sections are applicable to the deuteron-cesium interaction at the same relative velocity, hence at the deuteron energy of 1100 eV.

3.2.6 The Nuclear Spin Filter

A cross-section of the nuclear spin filter is shown in figure 6 . The main solenoid is divided into a central coil and two end coils, each separated by 3 sheets of 4.76 mm thick high permeability Conetic metal (this metal has a permeability of 8×10^4 μ_o, and a saturation field of 0.6 T), with entrance and exit apertures of 40 mm. These sheets at both ends of the central coil help to provide a uniform axial magnetic field within the nuclear spin filter. The end coils help to reduce the variations in the axial field at the apertures, as well as to provide a smooth transition from the low fields in the cesium canal and argon canal regions to the relatively high fields in the spin filter.

Figure 6. Nuclear spin filter assembly.

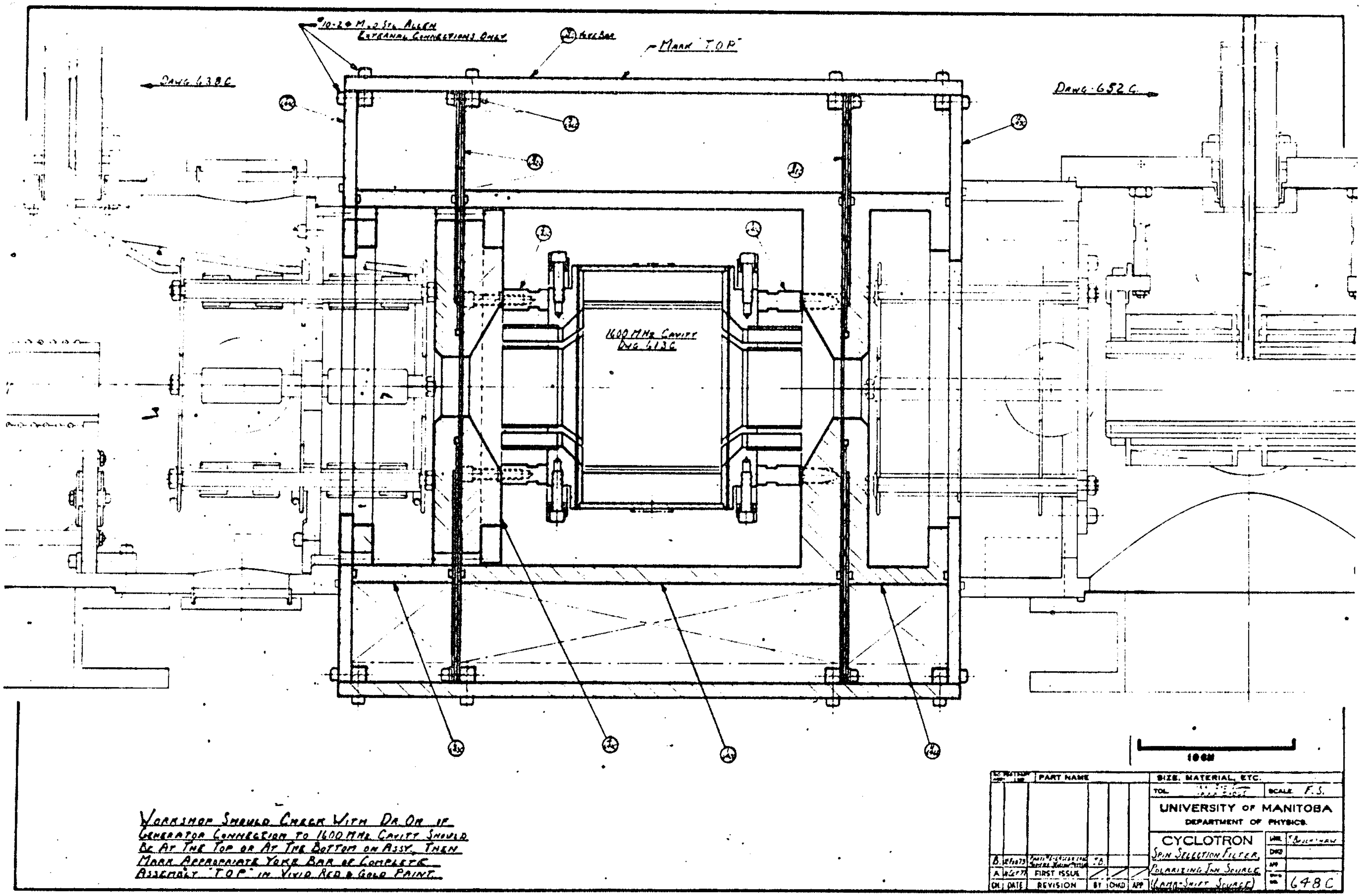

#10-24 M. O. Str. Allen
External Connections Only
Mark "TOP"
Dwg. 638C
Dwg. 652C
1600 MHz Cavity
Dwg. 613C
Workshop Should Check With Dr. Ott if
Generator Connection to 1600 MHz Cavity Should
Be At The Top or At The Bottom on Assy. Then
Mark Appropriate Yoke Bar of Complete
Assembly "TOP" in Vivid Red & Gold Paint.
10 CM
PART NAME
SIZE, MATERIAL, ETC.
TOL.
SCALE F.S.
UNIVERSITY OF MANITOBA
DEPARTMENT OF PHYSICS
CYCLOTRON
Spin Selection Filter
Polarizing Ion Source
(Lamb-Shift Source)
A
FIRST ISSUE
CH. DATE
REVISION
BY
CHKD
APP
648C

Two small trim coils were added onto the central coil for fine adjustment of the axial field uniformity.

The resonant cavity for the spin filter is similar in design to the cavity used in the Los Alamos polarized triton source. It is essentially a short cylindrical resonator which is driven in the TM_{010} mode at 1.600 GHz. This produces the oscillating axial electric field which couples the $2S_{1/2}$, $m_J = 1/2$ and the $2P_{1/2}$, $m_J = 1/2$ states. The amplitude of this field is adjusted by a variable attenuator. The field strength tends to drift immediately after starting the whole source but these drifts appear to be due to temperature changes in the resonant cavity. Once the body of the ion source comes to thermal equilibrium, the field strength is sufficiently stable. The resonant cavity is split axially into four quadrants. One pair of opposing sides is grounded, and has the transmitting loop for the radio frequency oscillator on one side, and a small pickup loop for field strength monitoring on the other side. The second pair of opposing sides can be biased up to ±300 V to produce a transverse static electric field to mix the $2S_{1/2}$, $m_J = -1/2$ and the $2P_{1/2}$, $m_J = 1/2$ states. During normal operation, about 5 mW of the 1.600 GHz oscillator is sufficient to drive the axial field, and a 250V potential difference is adequate to produce the required transverse static field.

3.2.7 The Argon Canal

After passage through the nuclear spin filter, the beam passes on through the argon canal shown in figure 7 . Here the electron attachment process:

$$H(2S) + Ar \rightarrow H^- + Ar^+$$

occurs, producing a beam of polarized H^- ions from the polarized H(2S) atoms. Argon is selected not for the magnitude of the cross-section for this process but rather for the high cross-section relative to the competing process:

$$H(1S) + Ar \rightarrow H^- + Ar^+$$

The selectivity of the argon for preferentially converting the metastable atoms to negative ions has been measured by Roussel et al. (1977) at 500 eV. The cross-sections for the metastable atom conversion is 1.58×10^{-17} cm^2 with a 15 mrad acceptance detector, and 5.06×10^{-17} cm^2 with a 57.5 mrad acceptance detector. The comparable cross-sections for the conversion of ground state atoms are 0.25×10^{-18} cm^2 and 0.95×10^{-18} cm^2 respectively. Thus a selectivity by a factor of 50 to 60 can be achieved using argon gas. This selectivity drops quite rapidly with increasing energy, and is only 30 at 1.0 keV and about 12 at 1.5 keV. This selectivity is important since after the spin filter,

Figure 7. Argon canal assembly.

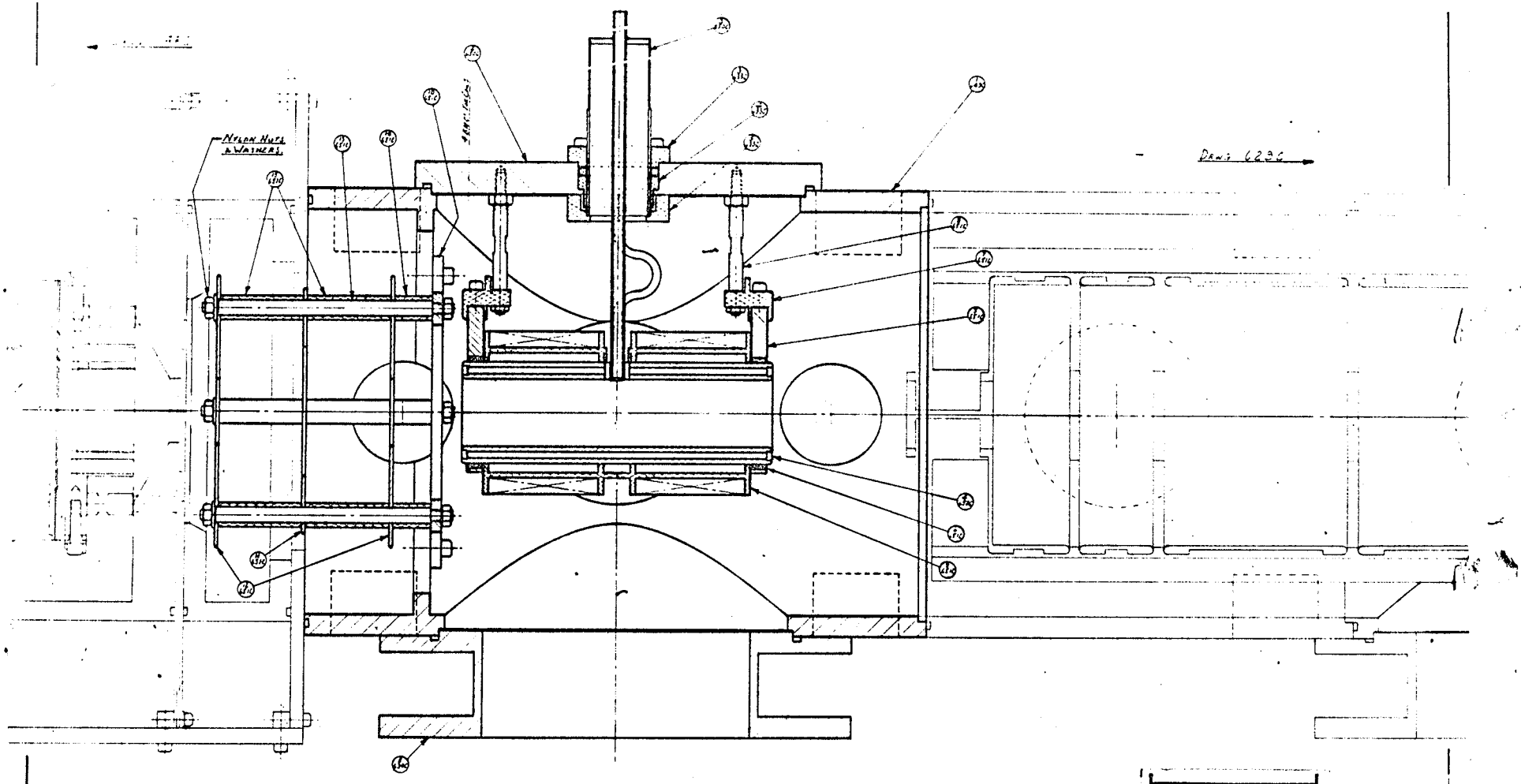

NO. REQ'D PER ASSY.	TOTAL NO. REQ'D	PART NAME	SIZE, MATERIAL, ETC.
			TOL. SCALE

UNIVERSITY OF MANITOBA
DEPARTMENT OF PHYSICS
CYCLOTRON

CH.	DATE	REVISION	BY	CHKD.	APP.
A		FIRST ISSUE			

DES.
DWN.
CHKD.
APP.
DATE
SHEET NO.

the intensity of the unpolarized H(1S) beam is about ten times that of the polarized H(2S) beam. After passage of the beam through the argon canal, the polarized component of the H^- beam is approximately four to five times the intensity of the unpolarized component. This relation can be used to accurately estimate the polarization of the H^- beam by the quench ratio technique to be described in Chapter 4. Argon gas is also used for the selective electron attachment to the polarized D(2S) atoms.

During normal operation, argon gas is slowly leaked into the canal through two needle valves. The gas escaping from the ends of the canal is pumped by a 203 mm (8 inch) cryopump located directly below the canal. The cryopump can continuously pump the argon for seven to eight days before it is necessary to shutdown the ion source to outgas the cryopump. This out-gassing procedure, and the startup of the ion source afterwards, takes about twelve hours.

An axial magnetic field with a strength up to 5 mT can be applied to the charge exchange region in the argon canal. This field helps to maintain an axial polarization axis, and in the case of state (2) or state (3) selection in deuterium, determines the vector and tensor polarization given by equation (2.14). The argon canal can also be biased up to -150 V with respect

to the body of the ion source.

3.2.8 The Decel-Accel Velocity Filter

The final stage of the polarized ion source is the decel-accel velocity filter which consists of the seven electrostatic cylinder lenses shown in figure 8 and four additional electrostatic cylinder lenses shown in figure 9 . The electric potentials of these lenses are set to initially decelerate the polarized H^- beam to under 100 eV and then to accelerate it to 11 keV, the injection energy of the cyclotron.

To understand the reasons for the initial deceleration it is necessary to discuss the origins of the most intense unpolarized background component. This background arises from two sequential electron attachment reactions, both occurring in the cesium canal, the first producing neutral hydrogen atoms and the second producing negative ions, as described in section 3.2.5. When the cesium vapor thickness is at the optimum value for polarized ion production, this H^- ion current is an order of magnitude greater than the polarized H^- component. To distinguish these two components of the total H^- current, the cesium canal is biased at +50 V with respect to the spin filter, and the argon cell is biased at -50 V with respect to the spin filter. Thus, neutral atoms produced at 550 eV in the cesium canal pass through to the argon canal at the same energy

Figure 8. First seven cylinder lenses of the decel-accel velocity filter.

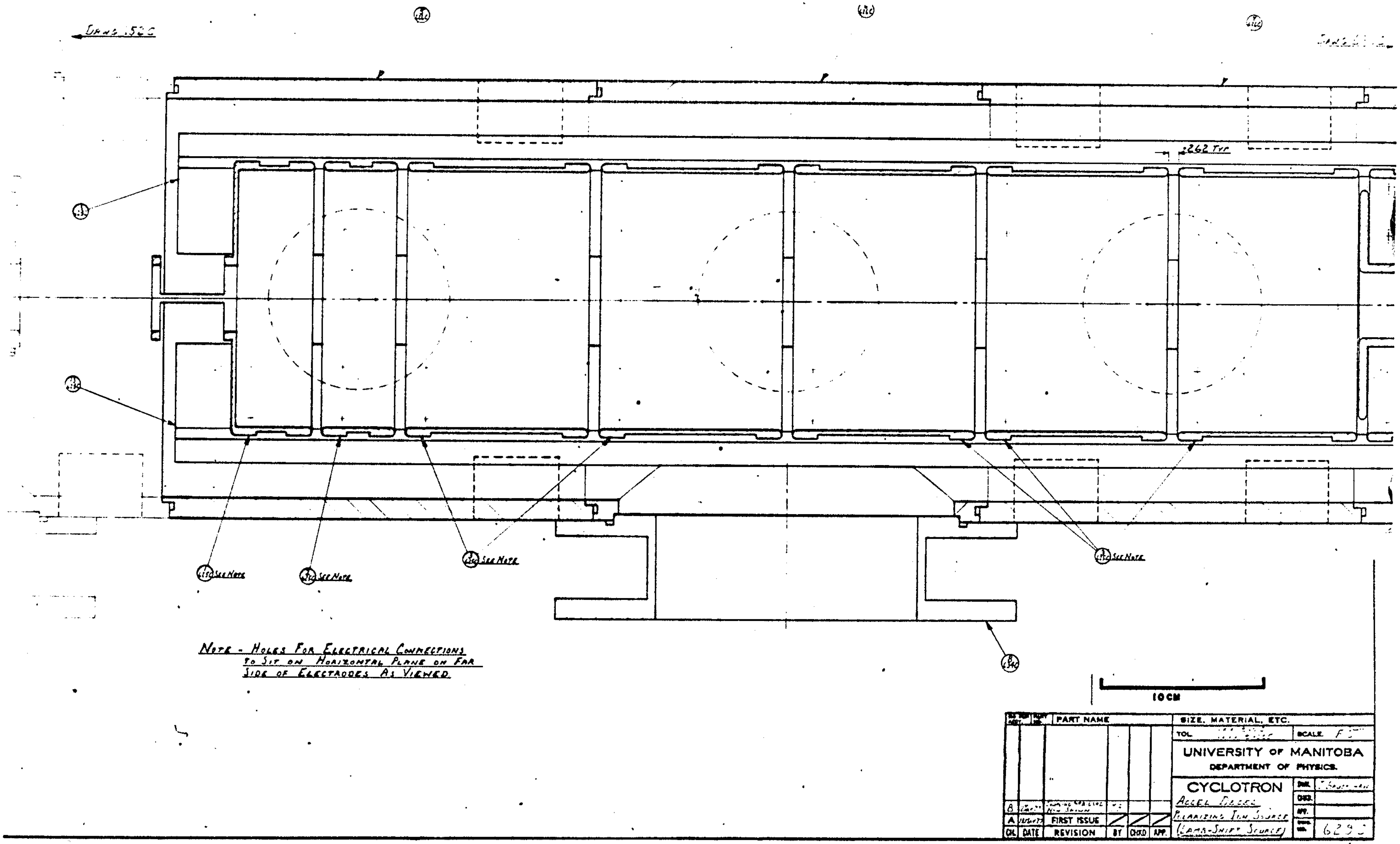

.262 TYP
SEE NOTE
NOTE - HOLES FOR ELECTRICAL CONNECTIONS TO SIT ON HORIZONTAL PLANE ON FAR SIDE OF ELECTRODES AS VIEWED
10 CM
PART NAME
SIZE, MATERIAL, ETC.
TOL.
SCALE
UNIVERSITY OF MANITOBA
DEPARTMENT OF PHYSICS
CYCLOTRON
ACCEL DECEL
POLARIZING ION SOURCE
(LAMB-SHIFT SOURCE)
A FIRST ISSUE
CH. DATE REVISION BY CHKD APP.

Figure 9. Last four cylinder lenses of the decel-accel velocity filter.

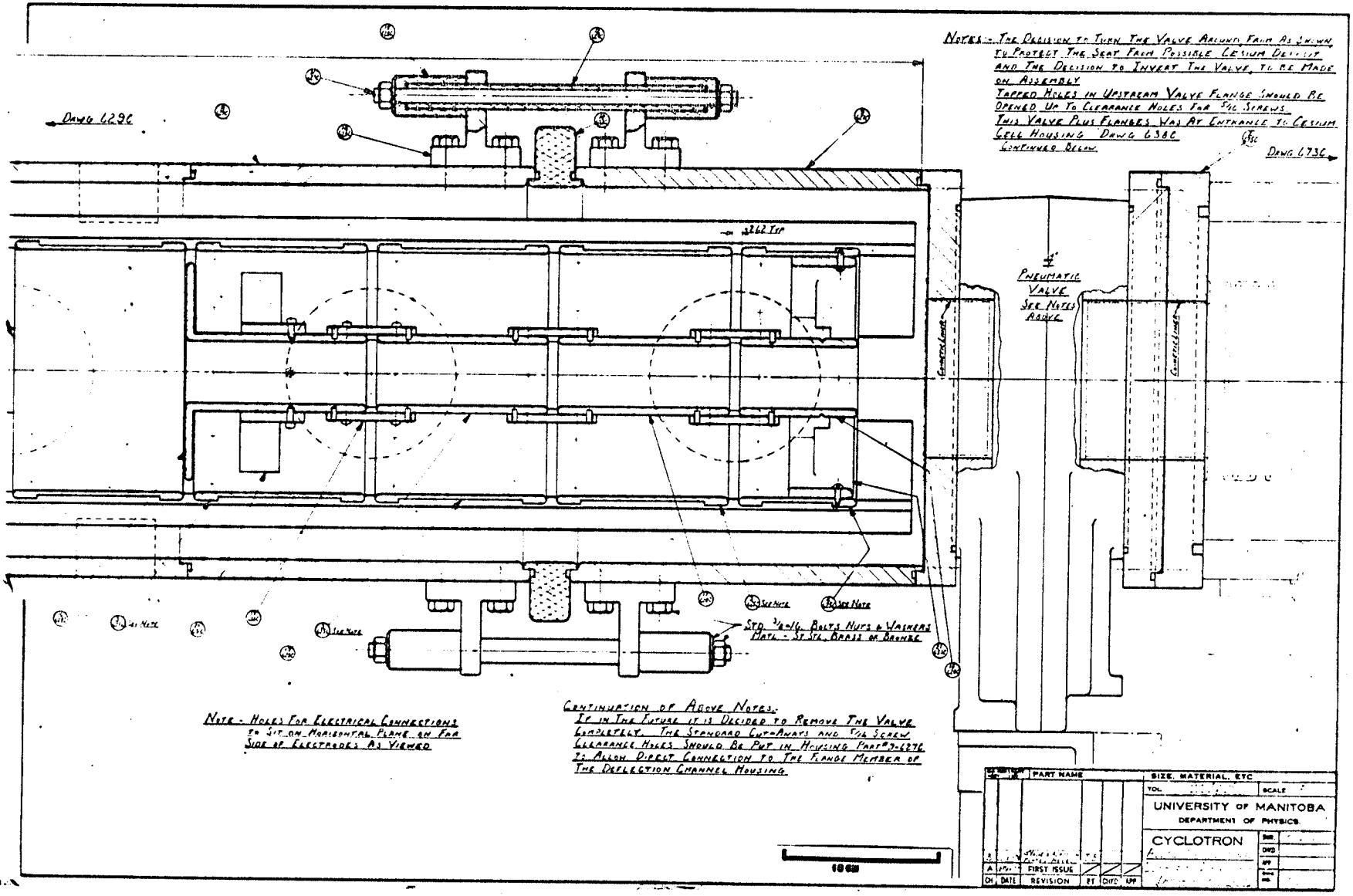
DWG 6296
DWG 6736
Notes - The Decision to Turn The Valve Around From As Shown To Protect The Seat From Possible Cesium Deposit And The Decision to Invert The Valve To Be Made On Assembly
Tapped Holes in Upstream Valve Flange Should Be Opened Up To Clearance Holes For 5/16 Screws.
This Valve Plus Flanges Was At Entrance To Cesium Cell Housing Dwg 6386
Continued Below
Pneumatic Valve See Notes Above
Std 3/8-16 Bolts Nuts & Washers Matl - St Stl, Brass or Bronze
Note - Holes For Electrical Connections To Sit On Horizontal Plane On Far Side of Electrodes As Viewed
Continuation of Above Notes.
If in The Future it is Decided to Remove The Valve Completely. The Standard Cut-Aways and 5/16 Screw Clearance Holes Should Be Put in Housing Part #7-6276 To Allow Direct Connection to The Flange Member of The Deflection Channel Housing
PART NAME
SIZE, MATERIAL, ETC
UNIVERSITY OF MANITOBA
DEPARTMENT OF PHYSICS
CYCLOTRON
FIRST ISSUE
DATE
REVISION

but negative ions produced in the cesium canal pass through a decelerating potential difference of 100 V. Hence the energy of the H^- ions produced in the cesium canal is only 450 eV at the argon whereas the polarized H^- ions are formed with an energy of 550 eV. Thus, by decelerating the polarized H^- beam to under 100 eV, the unpolarized component is completely stopped, i.e. the unpolarized component is completely defocussed into the lenses. The polarized component can then be accelerated to the injection energy.

This is the first time that this longitudinal deceleration technique for removing the unpolarized H^- background has been applied to polarized H^- Lamb-shift ion sources. The conventional technique is to apply a transverse electric field between the cesium canal and the nuclear spin filter which is strong enough to deflect the unpolarized H^- beam out of the neutral beam, but weak enough so that it does not quench the metastable beam. The conventional technique is very sensitive to the emittance of the neutral and charged beams. Good separation of these two beams with only a small transverse field of 500 V/m requires a small emittance for both beams. This is not always possible. By comparison, the longitudinal deceleration technique used in the U of M source uses only a longitudinal field $\lesssim$ 500 V/m, and the technique is virtually independent of the emittance

of the two beams.

3.2.9 The Polarized Ion Injection Beam Line

When the polarized beam emerges from the velocity filter, the beam is travelling horizontally with the spin polarization axis along the beam axis. For axial injection however, the beam must be injected vertically down into the cyclotron with the spin axis vertical. Thus, both the beam and the spin polarization axis must be rotated by 90°.

To do this, the beam is first bent through 90° horizontally by a 90° electrostatic deflector shown in figure 10 . Since the spin axis is unaffected by the electrostatic fields, the axis is now perpendicular to the beam direction, but still in the horizontal plane. The beam then passes axially through a solenoid which precesses the spin through 90° transverse to the beam direction. Now the spin axis is vertical. Another 90° electrostatic deflector is then used to deflect the beam down into the main axial injection system of the University of Manitoba cyclotron (see Batten et al., 1976). Both deflection channels produce very strong focussing in the deflection plane without any focussing in the transverse plane. Thus additional electrostatic focussing was necessary to compensate for these effects. The four electrostatic cylinder lenses from the velocity filter shown in figure 9 were replaced by an electro-

Figure 10. The first 90° electrostatic deflection channel.

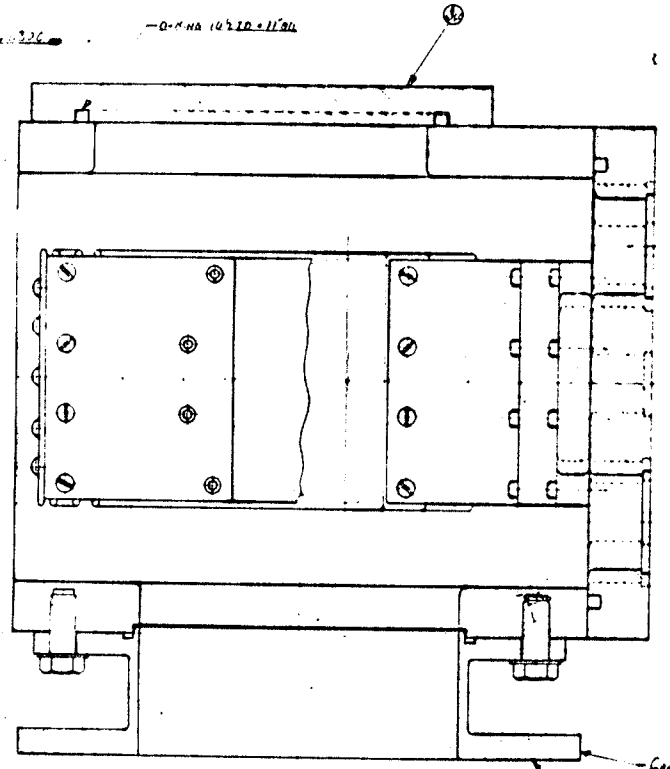

— Sectional Front View —

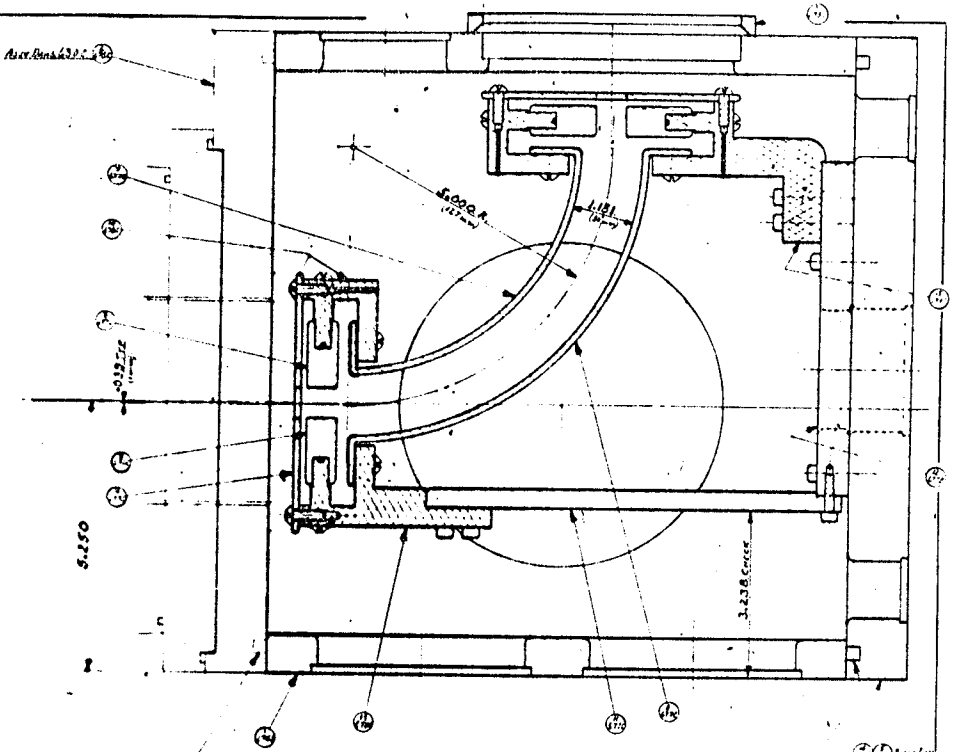

— Sectional Plan View —

Note: Required to See On On About Developing Bends at Top & Bottom of the Two ½ Cm. Deflection Channel Pieces Parts # 7 & 8 - 1772 C
Co-metic to be Fastened to Outer Faces of These Two Pieces

PART NAME	SIZE MATERIAL, ETC
	TOL. SCALE
UNIVERSITY OF MANITOBA DEPARTMENT OF PHYSICS	
CYCLOTRON	DWG.

LH	DATE	REVISION	BY	CHKD	APP
A		FIRST ISSUE			

static quadrupole doublet, and electrostatic quadrupole triplets were placed immediately before and after the spin precession solenoid. These lenses provided the additional focussing necessary to transport the polarized beam from the ion source to the axial injection system. Over 90% of the polarized beam could be transported to a current monitor 1 m above the yoke of the cyclotron, and typically over 70% to the electrostatic mirror located in the center of the cyclotron.

3.3 Ion Source Operation

Under the typical duoplasmatron operating conditions of 8 A arc current, 10 A magnet current, and a hydrogen gas pressure of 130 Pa (about 1 Torr), 0.7 mA of positive current was extracted and focussed into the cesium canal. Of this current, usually 60% were H^+ ions. The extractor voltage was 7 kV, and the second high voltage lens was about 3 kV. When operating with deuterium gas under the same duoplasmatron conditions only 0.4 mA of positive current was incident upon the cesium canal. To obtain even this current it was necessary to increase the extractor voltage to between 10 and 12 kV. The second high voltage lens was also increased slightly. These currents are substantially less than the 1 to 5 mA extracted current reported by other groups, but an increase in the current

onto the cesium canal above these values did not increase the total output of the polarized ion current.

The cesium canal's temperature would stabilize within an hour of commencing operation, but if the cesium canal had just been cleaned and filled, then the output from the source would steadily increase for almost 24 h. The nuclear spin filter magnet was then turned on, and argon gas was bled into the argon canal. The pressure in the region was increased from the base pressure of 0.06 mPa to 2,7 mPa (2×10^{-5} Torr). The H^- current produced consisted of largely negative ions formed from all four hyperfine metastable states. The beam transport system to the cyclotron was adjusted to maximize the total current. The cesium and argon canals' biases were then applied. If these biases were exactly equal in magnitude and opposite in polarity, the energy of the H^- beam formed from neutral hydrogen atoms passing through the argon canal remained unchanged. Consequently, the whole injection system remained tuned for these ions. However, the typical 100 eV shift in the energy of the H^- ions formed in the cesium canal was sufficient to completely detune the injection line for these background ions. This elimination of the background was usually so effective that it was unnecessary to adjust the velocity filter to stop this beam. Hence the velocity filter was usually simply adjusted for max-

imum transmission, and little attention was paid to the unpolarized H^- beam. The nuclear spin filter static and oscillating fields were then set and the spin filter magnetic field adjusted for the exact resonance desired. The static transverse field in the spin filter helped to further reduce the transmission of the unpolarized H^- beam from the cesium canal by deflecting it.

Once the ion source was adjusted 100 nA of polarized H^- or D^- beam was available after the first 90^o deflection channel. If, at any time unpolarized beam was desired, the spin filter static field was turned off, and the cesium and argon canals' biases were reduced to zero. Then between 1 and 3 μA of unpolarized H^- or D^- beam was available. In the case of polarized deuterons, the different states were selected by manually retuning the nuclear spin filter magnet.

CHAPTER 4

POLARIZED PROTON AND DEUTERON MEASUREMENTS

4.1 Introduction to Polarization Measurement Techniques

The most reliable technique for measuring nuclear polarization is through an appropriately chosen nuclear scattering experiment. Since experimentally this is virtually the same situation as measuring unknown analyzing tensors with beams of known polarization, the techniques developed by Ohlsen and Keaton (1973) for the latter case can be conveniently applied to the former case. The Cartesian coordinate system used to describe the state of the polarization is with the z-axis along the direction of the incident beam's momentum $\vec{k}_i$, the y-axis parallel to $\vec{k}_i \times \vec{k}_f$ where $\vec{k}_f$ is the detected scattered particle's momentum, and the x-axis is in the direction necessary to produce a right-handed coordinate system.

The differential cross-section for polarized proton scattering is given by:

$$I(\theta) = I_o(\theta)(1 + p_y A_y(\theta)) \qquad (1)$$

where $I_o(\theta)$ is the differential cross-section for unpolarized proton scattering, p_y is the y-component of the

beam polarization, and $A_y(\theta)$ is the vector analyzing power. The effect of p_y and A_y being non-zero is to produce a left-right asymmetry $\varepsilon = p_y A_y(\theta)$ in the count rate between two identical detectors placed at angle θ on opposite sides of the incident beam.

However, in practice the two detectors cannot be made to be completely identical, so the following procedure (see Ohlsen and Keaton, 1973) is used. A run is made with a polarization p_y incident upon the target producing L_1 counts in the left detector and R_2 counts in the right detector. The polarization is then reversed, i.e. $p_y \rightarrow -p_y$, and a second run is taken, producing R_1 counts in the left detector and L_2 counts in the right one. The geometric means:

$$\begin{aligned} L &= (L_1 L_2)^{1/2} \\ R &= (R_1 R_2)^{1/2} \end{aligned} \qquad (2)$$

are then formed, and the asymmetry ε is then given by:

$$\varepsilon = \frac{L - R}{L + R} = p_y A_y(\theta) \qquad (3)$$

which is independent of first-order instrumental asymmetries. If the target nucleus is selected such that at some angle $A_y(\theta)$ is both large and known accurately, an accurate determination of p_y can be made.

The situation with polarized deuterons is more complex for the general scattering case. Since the

determination of the incident beam polarization is of interest here, only the special case in which the spin polarization axis is parallel to the y-axis will be considered. In this case the differential cross-section is:

$$I(\theta) = I_o(\theta)(1 + \frac{3}{2}p_y A_y(\theta) + \frac{1}{2}p_{yy}A_{yy}(\theta)) \qquad (4)$$

where again $I_o(\theta)$ is the differential cross-section for unpolarized deuterons, $A_y(\theta)$ is the vector analyzing power, and $A_{yy}(\theta)$ is one component of the tensor analyzing power. However, reversing the sign of p_y does not affect p_{yy}. Thus if an asymmetry ε is evaluated as in the case for protons, the result is:

$$\varepsilon = \frac{\frac{3}{2}\, p_y A_y(\theta)}{1 + \frac{1}{2}\, p_{yy}A_{yy}(\theta)} \qquad (5)$$

To evaluate $p_{yy}A_{yy}(\theta)$, the sum of the counts in the left and right detectors, normalized to n, the number of deuterons passing through the target, and to N, the number of target nuclei, is formed:

$$T_{pol} = (L_{pol} + R_{pol})/nN \qquad (6)$$

A similar sum is formed when the incident beam is unpolarized giving:

$$T_{un} = (L_{un} + R_{un})/nN \qquad (7)$$

Then:

$$p_{yy}A_{yy}(\theta) = 2\left[\frac{T_{pol}}{T_{un}} - 1\right] \qquad (8)$$

This value is then substituted into equation (5) to evaluate $p_y A_y(\theta)$. Unfortunately, this technique is very sensitive to possible normalization errors in equation (6) and (7).

Indirect techniques also sometimes exist for the measurement of the polarization. One of the advantages of the nuclear spin filter type of polarized ion source is that the maximum polarization of the beam may be easily determined by the quench ratio technique described by Ohlsen (1970). This technique relies on the assumption that the total polarized beam from the source consists of two components: the polarizable component whose polarization is given exactly by equations (2.13) and (2.14), and a completely unpolarized background from ground state atoms converted to negative ions in the argon canal. Introducing the quench ratio, Q, as the ratio between the total current from the source and the unpolarized background current, the maximum polarizations of the beam on target, p_y' and p_{yy}', are given by:

$$\begin{aligned} p_y' &= (1 - 1/Q)p_y \\ p_{yy}' &= (1 - 1/Q)p_{yy} \end{aligned} \qquad (9)$$

where p_y and p_{yy} are obtained from equation (2.13) or (2.14). The Los Alamos group (Ohlsen, 1970) have shown that if the quench ratio on the target is used then the ion source and spin precessor can be adjusted so that the agreement between the quench ratio and the nuclear scattering techniques is better than ±0.01 for both p_y and p_{yy}. The convenience of the quench ratio technique is that, once properly adjusted, a polarization monitor upstream or downstream from the target is unnecessary for most work.

4.2 Deuteron Polarization Measurements

The measurement of the deuteron polarization was made in conjunction with an experiment measuring the angular distribution of A_y and A_{yy} for the reaction $^4He(\vec{d},d)^4He$ at 12.6 MeV incident deuteron energy. The apparatus and results of the experiment are described in detail by Birchall et al. (1981) so only a brief outline will be given here. Polarized D^- ions were accelerated by the U of M cyclotron, extracted at an energy of 12.8 MeV and transported to a target cell containing ^4He gas at a pressure of 102 kPa. The deuteron energy at the center of the cell was 12.6 MeV. The current passing through the target was ∿100 pA on the average, and was either monitored by a Keithley Model 610R electrometer or integrated using a Brookhaven Instruments

Corporation Model 1000 current integrator. The elastically scattered deuterons were detected by two silicon surface-barrier detectors mounted on movable arms located on opposite sides of the scattering chamber. Elastic scattering measurements were taken with polarized deuterons from state (1) selection in the nuclear spin filter. The sign of p_y was reversed by reversing the polarity of the nuclear spin filter magnets. Since this does not change p_{yy}, measurements were also taken with unpolarized beam where $p_{yy} = 0$. The quantities $p_y A_y$ and $p_{yy} A_{yy}$ were evaluated using the techniques outlined in section 4.1. p_y and p_{yy} were between 0.75 and 0.80 as estimated by the quench ratio technique, and the values of A_y and A_{yy} at a laboratory scattering angle of 37.5° were derived. The value -0.685 ± 0.022 for A_y agrees well with the value -0.6941 ± 0.0091 measured by Schmelzbach et al. (1976) at the same energy and angle. The value for A_{yy} of 0.816 ± 0.091 is slightly below the value of 0.95 at 37.3° and 12.5 MeV which was taken from a graph in the paper by Grüebler et al. (1975). However, the possible normalization errors produced by integrating such a small beam current could account for this difference in A_{yy}. The excellent agreement in A_y indicates that the quench ratio polarization measurement technique is reliable to at least ± 0.03 in p_y at the U of M.

4.3 Proton Polarization Measurements

The measurements of the proton polarization were performed using the same apparatus as was used in the deuteron polarization measurements, except that silicon surface-barrier detectors with 2 mm depletion depths replaced the thinner detectors. The vector analyzing power for $^4He(\vec{p},p)^4He$ elastic scattering has been measured between 20 and 40 MeV in 2 MeV steps by Bacher et al. (1972) and shows that $A_y \geq 0.80$ at a laboratory scattering angle near 125° for almost all energies in that range. Hence, the two detectors were placed at equal angles in the region from 115° to 130°. The particular angle chosen depended upon where the maxima in A_y occurred for the particular proton energy used. The quantity $p_y A_y$ was determined using the techniques described in section 4.1.

Polarized H^- ions from state (1) were formed and accelerated in the cyclotron. The current passing through the scattering chamber was between 0.1 nA and 3.0 nA depending upon the cyclotron and beam transport operating conditions. The polarization was reversed by reversing the polarity of all the magnets in the nuclear spin filter. The sign of the polarization injected into the cyclotron was known from the polarity of the nuclear spin filter magnets and the spin precession magnet, and this assignment was confirmed by the polarization of the

deuterons.

The results of the proton polarization measurements indicated that there existed a severe polarization loss. Although the quench ratio measurements estimated p_y to be between 0.75 and 0.85, the elastic scattering data indicated that p_y could vary between -0.10 ± 0.02 and 0.10 ± 0.02. The negative sign indicates that the polarization in the scattering chamber was opposite to that injected into the cyclotron. There was also a large variation of the polarization in the phase space of the beam extracted from the cyclotron. In one case, reducing the size of the slits in the external beam transport system to cut down the beam phase space transmitted to the scattering chamber could increase p_y from 0.20 ± 0.04 to 0.43 ± 0.04. Yet, if the radio-frequency dee voltage were changed from 27 kV to 31 kV the same reduction in phase space changed p_y from -0.08 ± 0.02 to -0.22 ± 0.07. In general, almost any adjustment in the cyclotron's operation, such as the main magnetic field, the dee voltage amplitude, or the injection beam line parameters, could cause some change in the measured polarization. Most of the polarization loss, and its dependence on the cyclotron's operation can be explained by resonant depolarization during acceleration of the H^- ions in the cyclotron.

CHAPTER 5

RESONANT DEPOLARIZATION IN CYCLOTRONS

5.1 Introduction

There has been concern about the possible loss of polarization of polarized beams in cyclic particle accelerators for almost as long as polarized ion sources have existed. With the exception of linear accelerators, almost all accelerators capable of accelerating protons to more than 20 MeV rely on magnetic fields to confine the particles during acceleration. The magnetic fields in such accelerators, e.g. cyclotrons, synchrotrons, or synchro-cyclotrons, are usually spatially varying and sometimes temporally varying. Initially it was not clear under which circumstances the interaction of a particle's magnetic moment with the accelerator's magnetic field would lead to an effectively random reorientation of a particle's spin during acceleration.

The first complete review of possible depolarizing effects was by Froissart and Stora (1960) who discussed the conditions for depolarization of protons in a synchrotron. Their work has since been extended by some other groups, and especially by the group at the Argonne National Laboratory working on the Zero Gradient

Synchrotron (ZGS). (see Khoe et al., 1975) It was at the ZGS that significant depolarization was observed during acceleration, and that techniques for minimizing the depolarization in synchrotrons were developed. Later, a similar analysis of depolarization was developed for protons and deuterons in cyclotrons by Kim and Burcham (1964) and for protons in synchro-cyclotrons by Besnier (1970). These papers and others (for example Baumgartner and Kim, 1966) concluded that the loss of polarization of protons and deuterons was less than 1% for the synchro-cyclotrons and cyclotrons considered. By 1967 several cyclotrons had successfully accelerated polarized beams with no measureable loss of polarization, and it was generally concluded that depolarization was unlikely to be significant in any cyclotron. As indicated in Chapter 4, this is not the case at the University of Manitoba cyclotron.

This chapter will review and develop the theory of depolarization as applied to cyclotrons with particular emphasis on polarized H^- ions. First the relativistic spin equations of motion will be developed. Then a review of the phenomena of spin resonance will be presented. After this the motion of charged particles in a cyclotron will be reviewed and the coupling of the particle's spin motion and its spatial motion will be shown. These relations will then be applied to the situation in the

U of M cyclotron.

5.2 Spin Equations of Motion

Consider a particle with mass m and charge q, and with total angular momentum of $\hbar\vec{S}$ and a magnetic moment $\vec{M}$ of $g_I \mu_n \vec{S}$ where μ_n is the nuclear magneton:

$$\mu_n = \frac{e\hbar}{2m_p}$$

where m_p is the mass of the proton and e is the charge of the proton. If the particle is at rest in a magnetic field $\vec{B}$, the classical equation of motion for the spin $\vec{S}$ is:

$$\hbar \frac{d\vec{S}}{dt} = \vec{M} \times \vec{B} = g_I \mu_n \vec{S} \times \vec{B} \qquad (1)$$

In quantum mechanics, the equivalent equation of motion for the spin angular momentum operator $\vec{S}$ is:

$$\frac{\hbar}{i} \frac{d\vec{S}}{dt} = g_I \mu_n (\vec{S}(\vec{B}\cdot\vec{S}) - (\vec{B}\cdot\vec{S})\vec{S}) \qquad (2)$$

Although the two equations are quite different in appearance, it can be shown that the motion of the expectation value of the components of $\vec{S}$ in equation (2) is identical to the motion calculated in the classical case from equation (1) (see Slichter, 1978). Thus only the classical spin equations will be considered further.

The relativistic equations of motion must be a

relativistic generalization of equation (1), i.e. when the velocity of the particle is zero, the relativistic equation must reduce to equation (1). The details of the derivation are given in Jackson (1975) and lead to the equation:

$$\frac{dS^{\alpha}}{d\tau} = \frac{1}{\hbar} g_I \mu_n \left\{ F^{\alpha\beta} S_{\beta} + \frac{U^{\alpha}}{c^2} (S_{\lambda} F^{\lambda\mu} U_{\mu}) \right\} - \frac{U^{\alpha}}{c^2} \left(S_{\beta} \frac{dU^{\beta}}{d\tau} \right) \tag{3}$$

Here, U^{α} is the 4-velocity of the particle, $F^{\alpha\beta}$ is the antisymmetric electromagnetic 4-tensor, $\frac{d}{d\tau}$ is the derivative with respect to proper time, and c is the speed of light. In this equation the spin of the particle is represented by the 4-vector S^{α} which is related to the spin $\vec{s}$ by the relations:

$$S_0 = \gamma \vec{\beta} \cdot \vec{s}$$
$$\vec{S} = \vec{s} + \frac{\gamma^2}{\gamma + 1} (\vec{\beta} \cdot \vec{s}) \vec{\beta} \tag{4}$$

where S_0 is the time component of S^{α}, $\vec{S}$ is the space components of S^{α}, and $\vec{\beta}$, γ have the usual meaning in relativistic mechanics.

In order to solve equation (3) for the spin motion, the particle's motion must be known. If the electric and magnetic fields in space are sufficiently

smoothly varying, i.e. if the interactions of the particle's magnetic moment with the gradient of the magnetic field is so small that it does not affect the particle's motion, then the motion of the particle with mass m, and total charge q, is given by:

$$\frac{dU^{\alpha}}{d\tau} = \frac{q}{m} F^{\alpha\beta} U_{\beta} \tag{5}$$

Equation (3) then becomes:

$$\frac{dS^{\alpha}}{d\tau} = \left\{ g_I \mu_n F^{\alpha\beta} S_{\beta} + \frac{U^{\alpha}}{c^2} \left(S_{\lambda} F^{\lambda\mu} U_{\mu} \right) \left(g_I \mu_n - \frac{q}{m} \right) \right\} \tag{6}$$

which is known as the BMT equation (see Bargmann et al., 1959). Rewriting this equation in the usual space and time coordinates, recalling that $\mu_n = \frac{e\hbar}{2m_p}$, gives:

$$\begin{aligned} \frac{d\vec{s}}{dt} = \frac{q}{m} \vec{s} \times \Bigg\{ & \vec{B} \left(\frac{g_I}{2} \left(\frac{me}{m_p q} \right) - 1 + \frac{1}{\gamma} \right) \\ & - \vec{\beta} \times \vec{E} \left(\frac{g_I}{2} \left(\frac{me}{m_p q} \right) - \frac{\gamma}{\gamma + 1} \right) \\ & - \left(\frac{\gamma}{\gamma + 1} \right) \vec{\beta} (\vec{\beta} \cdot \vec{B}) \left(\frac{g_I me}{2 m_p q} - 1 \right) \Bigg\} \end{aligned} \tag{7}$$

Introducing the effective g-factor g′:

$$g' = g_I \left(\frac{me}{m_p q} \right) \tag{8}$$

equation (7) becomes:

$$\frac{d\vec{s}}{dt} = \frac{q}{m}\vec{s} \times \left\{\vec{B}\left(\frac{g'}{2} - 1 + \frac{1}{\gamma}\right) - \vec{\beta} \times \vec{E}\left(\frac{g'}{2} - \frac{\gamma}{\gamma + 1}\right)\right.$$
$$\left. - \left(\frac{\gamma}{\gamma + 1}\right)\vec{\beta}(\vec{\beta} \cdot \vec{B})\left(\frac{g'}{2} - 1\right)\right\} \qquad (9)$$

where $\vec{B}$, $\vec{E}$ are the magnetic and electric fields as measured in the laboratory reference frame and $\vec{s}$ is the spin vector.

5.3 Nuclear Magnetic Resonance

The solution of equation (1) for the motion of a spin $\vec{s}$ in a uniform magnetic field $\vec{B}$, assumed to be along the z-axis, is:

$$\begin{aligned} s_z &= s\cos(\psi) \\ s_x &= s\sin(\psi)\cos(-g_I\mu_n Bt/\hbar) \\ s_y &= s\sin(\psi)\sin(-g_I\mu_n Bt/\hbar) \end{aligned} \qquad (10)$$

where ψ is the angle between $\vec{s}$ and the z-axis, $s = |\vec{s}|$, and $B = |\vec{B}|$. The equations of motion for $\vec{s}$ correspond to a rotation of $\vec{s}$ about the z-axis with a constant angular velocity of $\Omega_o = -\frac{1}{\hbar}g_I\mu_n B$. This is known as the Larmor precession of the spin in a magnetic field.

If in addition to the main magnetic field $\vec{B}$ a magnetic field $\vec{B}_1$ is applied perpendicular to $\vec{B}$ and rotating in the x-y plane with angular velocity Ω, then the phenomenon of magnetic resonance may occur (see Slichter, 1978). Now equation (1) is:

$$\frac{d\vec{s}}{dt} = \frac{1}{\hbar} g_I \mu_n \vec{s} \times (B\hat{k} + B_1(\hat{i}\sin(\Omega t) + \hat{j}\cos(\Omega t))) \qquad (11)$$

This can be solved by a transformation to a coordinate system rotating with an angular velocity of Ω about the z-axis, i.e. to the coordinate system where $\vec{B}_1$ is fixed, thus:

$$\left.\frac{d\vec{s}}{dt}\right|_{rot} = g_I \mu_n \vec{s} \times (B\hat{k} + B_1\hat{i}) + (\vec{s} \times \Omega\,\hat{k}) \qquad (12)$$

Now there is no time dependence on the right hand side of equation (12) and the solution is a precession of $\vec{s}$ about an effective magnetic field of:

$$\vec{B}_{eff} = (B + \frac{\Omega\hbar}{g_I \mu_n})\hat{k} + B_1\hat{i} \qquad (13)$$

These conditions are shown in figure 11 . As long as

$$\left|B + \frac{\Omega\hbar}{g_I \mu_n}\right| >> B_1 \qquad (14)$$

then $\vec{B}_{eff}$ is almost parallel to $\vec{B}$ and so the initial spin orientation does not change significantly. However magnetic resonance occurs when equation (14) is no longer valid. Then:

$$\Omega \sim -Bg_I \mu_n \frac{1}{\hbar} = \Omega_o \qquad (15)$$

and $\vec{B}_{eff}$ will no longer be essentially along the z-axis. In particular, if $\Omega = \Omega_o$ then:

Figure 11. The effective magnetic field, $\vec{B}_{eff}$, in magnetic resonance.

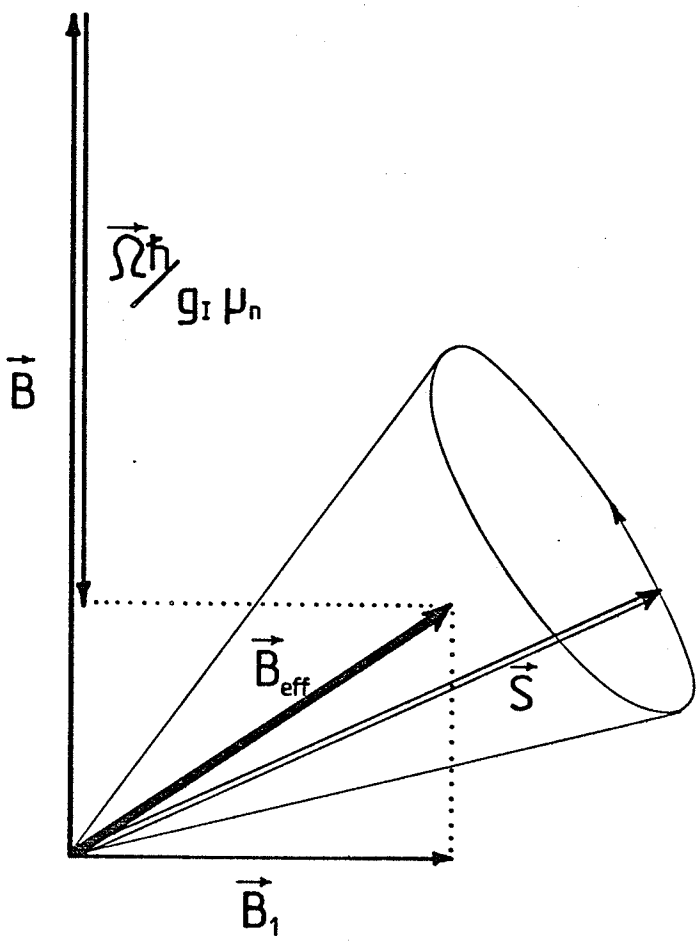
$\vec{\Omega}\hbar / g_I \mu_n$
$\vec{B}$
$\vec{B}_{eff}$
$\vec{S}$
$\vec{B}_1$

$$\vec{B}_{eff} = B_1 \hat{i} \tag{16}$$

and the precession is about the x-axis in the rotating frame, with a frequency of $\frac{-1}{\hbar} B_1 g_I \mu_n$, and s_z varies as:

$$s_z = s \cos(-g_I \mu_n B_1 t/\hbar) \tag{17}$$

The condition for magnetic resonance can occur during acceleration of polarized particles in a cyclotron, and hence there may be a decrease or loss of polarization. However, a description of the magnetic fields and the motion of charged particles within a cyclotron is necessary before giving a quantitative discussion of the polarization loss.

5.4 Particle Motion in a Sector-Focussed Isochronous Cyclotron

When a particle of mass m, charge q and momentum $\vec{p}$ is placed in a magnetic field $\vec{B}$, it experiences the Lorentz force given by:

$$\frac{d\vec{p}}{dt} = \frac{q}{\gamma m} (\vec{p} \times \vec{B}) \tag{18}$$

If $\vec{B}$ is uniform and $\vec{p}$ is perpendicular to $\vec{B}$, then the solution to equation (18) is a circular orbit in a plane normal to $\vec{B}$ of radius $r = |p|/(qB)$ and the particle moves with constant angular velocity:

$$\omega_c = \frac{qB}{\gamma m} \tag{19}$$

known as the cyclotron frequency.

The magnetic field of a sector-focussed cyclotron with N sectors is symmetric with respect to a median plane normal to the z-axis, and also has N-fold symmetry about the z-axis. Thus the vertical field in the median plane may be described by the following Fourier expansion:

$$B_z(r,\theta) = B(r)(1 + \sum_{n=1}^{\infty}(a_n \sin(n\theta) + b_n \cos(n\theta))) \qquad (20)$$

where a_n and b_n are only significantly non-zero for n an integral multiple of N. Sometimes the ideal cyclotron field will deviate from perfect N-fold symmetry in the center region, and at the largest radii for extraction. For most of this discussion these deviations are not significant. The cyclotron frequency is given by:

$$\omega_c = \frac{q}{m} B(0) \qquad (21)$$

The requirement for an isochronous cyclotron that the frequency be independent of the energy of the ion constrains B(r) to slowly increase as the radius increases. This is to compensate for the effective mass increase from relativistic effects as the energy increases.

To discuss the properties and stability of the ions' orbits, it is convenient to introduce the concept of equilibrium orbits (EO). An EO of energy E is a possible particle trajectory having the same N-fold symmetry as the magnetic field when there is no acceler-

ating voltage applied to the dees. This EO permits the introduction of the coordinate system, shown in figure 12 , for the arbitrary trajectory of a particle with energy E. An orbit produced by initially displacing a particle from its EO is said to be stable if the displacement between the two orbits remains bounded. Some of the general conditions for orbit stability in cyclotrons and other similar accelerators are discussed in more detail in Hagedoorn and Verster (1962), or Livingood (1961).

Stability with respect to small perturbations of the orbit in the z-direction is produced by the focussing effects of the small transverse magnetic fields above or below the median plane. Although no magnetic fields transverse to the z-axis exist in the median plane, such fields can be present for small displacements from the plane. A Taylor series expansion of the transverse fields about the median plane yields:

$$B_x \simeq B_r = \frac{\partial B_z}{\partial r} z + \frac{\partial^2 B_z}{\partial r^2} zx + \ldots$$

$$B_y \simeq B_\theta = \frac{1}{r}\frac{\partial B_z}{\partial \theta} z + \frac{1}{r}\frac{\partial^2 B_z}{\partial \theta \partial r} zx + \ldots \qquad (22)$$

using the relation $\vec{\nabla} \times \vec{B} = 0$. The vertical motion (see Hagedoorn and Verster, 1962) produced by these fields is nearly periodic with a frequency of $\nu_z \omega_c$ where ν_z is the vertical betatron tune or frequency.

Figure 12. The coordinate system used on an equilibrium orbit (EO).

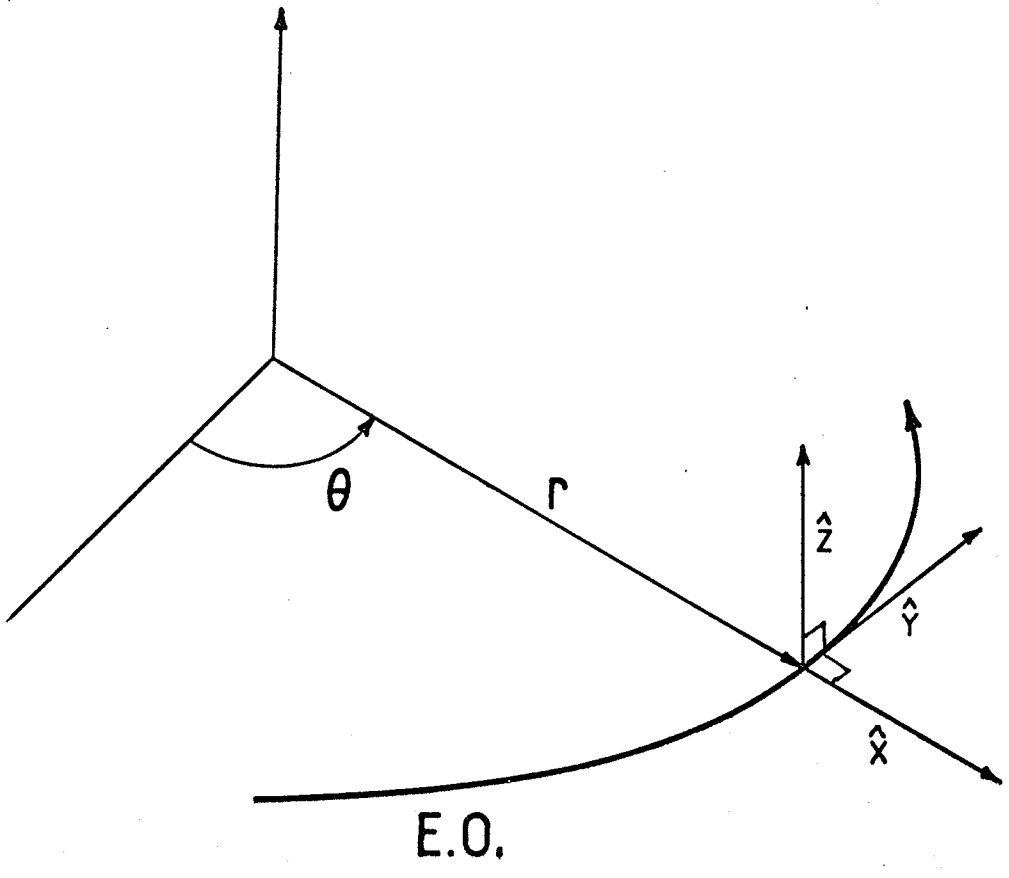
θ
r
$\hat{Z}$
$\hat{Y}$
$\hat{X}$
E.O.

This motion can be well approximated by:

$$z(t) = z_m \cos(\nu_z \omega_c t + \phi_o) \qquad (23)$$

Similarly, there is a radial focussing effect providing stability of the orbits which are displaced radially by a small amount x from the EO. This motion is also almost periodic with a frequency of $\nu_r \omega_c$, where ν_r is the radial betatron tune or frequency. In isochronous cyclotrons, ν_r is usually close to but greater than 1. Hence the time dependence of the radial deviation from the EO can be also approximated by:

$$x(t) = x_m \cos(\nu_r \omega_c t + \phi_1) \qquad (24)$$

Thus the general motion of an ion in a sector-focussed isochronous cyclotron is one of approximately circular motion of angular velocity $\omega_c = qB_o/m$ where $B_o = B(0)$, with additional small vertical and radial betatron oscillations. The effects of the acceleration of the ions is to produce a smooth change in the radius, ν_z and ν_r as the energy increases.

5.5 Spin Motion in a Sector-Focussed Cyclotron

Before using equation (9) to describe the spin motion in the cyclotron it is necessary to transform equation (9) into a more convenient coordinate system. A transformation to a reference frame which, when viewed

from the laboratory frame, rotates at the cyclotron frequency is given by:

$$\left.\frac{d\vec{s}}{dt}\right|_{rot} = \left.\frac{d\vec{s}}{dt}\right|_{lab} - \vec{s} \times \omega_c \hat{k} \tag{25}$$

where all the quantities are observed in the laboratory frame. Introducing the independent variable $\theta = \omega_c t$, and neglecting the effects of any electric fields gives the spin motion equation, $\frac{d\vec{s}}{d\theta}$, in a rotating frame:

$$\frac{d\vec{s}}{d\theta} = \vec{s} \times \left(\frac{1}{\gamma B_o}\right)\left\{\vec{B}(\gamma G + 1) - \frac{\vec{\beta}(\vec{\beta}\cdot\vec{B})}{\beta^2} G(\gamma - 1) - \gamma B_o \hat{k}\right\} \tag{26}$$

where $G = (\frac{g}{2} - 1)$. The first term is the intrinsic spin precession. The second term contains the component of $\vec{B}$ in the direction of motion multiplied by $G(\gamma - 1)$ and is a relativistic correction. The third term is simply a consequence of the reference frame transformation.

Let $\vec{p} = (p_x, p_y, p_z)$ be the momentum of the particle, then:

$$\frac{\vec{\beta}(\vec{\beta}\cdot\vec{B})}{\beta^2} = \frac{\vec{p}(\vec{p}\cdot\vec{B})}{p^2} \tag{27}$$

Now equation (26) can be written as:

$$\frac{d\vec{s}}{d\theta} = \vec{s} \times \frac{1}{\gamma B_o}\left\{\left\{B_z(\gamma G + 1) - \gamma B_o - p_z\frac{(\vec{p}\cdot\vec{B})}{p^2} G(\gamma - 1)\right\}\hat{k}\right.$$

$$+ \left[B_x(\gamma G + 1) - p_x \frac{(\vec{p}\cdot\vec{B})}{p^2} G(\gamma - 1)\right]\hat{i} \qquad (28)$$

$$+ \left[B_y(\gamma G + 1) - p_y \frac{(\vec{p}\cdot\vec{B})}{p^2} G(\gamma - 1)\right]\hat{j}\Bigg]$$

Introducing $\vec{b} = \vec{B}/\gamma B_o$, the spin motion for an ion on the EO is given by:

$$\frac{d\vec{s}}{d\theta} = \vec{s} \times (b_z(\gamma G + 1) - 1)\hat{k} \qquad (29)$$

This is simply a precession about the z-axis with a θ dependent frequency of:

$$\Omega = \omega_c \gamma G + \omega_c(\gamma G + 1) \sum_{n=1}^{\infty} (a_n \sin(n\theta) + b_n \cos(n\theta)) \qquad (30)$$

The second term is a modulation of the main precession frequency, $\Omega_o = \omega_c \gamma G$, at multiples of the N-fold symmetry of the magnetic field. The effect of this frequency modulation will be neglected for the moment and will be discussed later. Thus, the basic motion of the spin in the particle's reference frame is a precession at γG times the cyclotron frequency. The positive or negative sign of G determines whether the sense of the precession is in the same or the opposite direction to the ion's rotation in the cyclotron.

If terms in equation (28) which are of first order in z and $\frac{dz}{dt}$ are now included, the spin motion equations become:

$$\frac{d\vec{s}}{d\theta} = \vec{s} \times \left\{\gamma G\hat{k} + b_x(\gamma G + 1)\hat{i} + (b_y(G + 1) - \frac{p_z}{p} b_z G(\gamma - 1))\hat{j}\right\} \tag{31}$$

where the p_z term is included since:

$$\frac{p_z}{p} = \frac{\gamma m}{p} \frac{dz}{dt} \simeq - \frac{\nu_z}{R} z_m \sin(\nu_z \omega_c t + \phi_o) \tag{32}$$

which is of the same order of magnitude as z. Since the last term, $p_z b_z G(\gamma - 1)/p$, in equation (31) is much smaller than the others for low energy cyclotrons such as the U of M cyclotron, it will be neglected. In high energy accelerators where relativistic effects cannot be neglected, and ν_z is not small, this term can easily be as large as the other terms.

For convenience, introduce the vector $\vec{\sigma}$ in the x-y plane such that equation (31) can be written as:

$$\frac{d\vec{s}}{d\theta} = \vec{s} \times \gamma G\hat{k} + \vec{s} \times \vec{\sigma}z \tag{33}$$

Since $\vec{\sigma}$ is a vector in the two dimensional x-y plane, it may be represented by a complex quantity:

$$\sigma = \sigma_x + \imath\sigma_y \tag{34}$$

where:

$$\sigma_x z = b_x(\gamma G + 1)$$

$$\sigma_y z = b_y(G + 1)$$

For isochronous cyclotrons, $\gamma B_o \simeq B(R)$ where R is the average radius of the EO corresponding to γ. From Hagedoorn and Verster (1962), the error in this approximation is of second order in the magnitude of the coefficients a_n and b_n. Hence σ_x and σ_y can be expanded in the following Fourier series:

$$\sigma_x = (\gamma G + 1)\left\{\frac{B'(R)}{B(R)}\left(1 + \sum_{n=1}^{\infty}(a_n \sin(n\theta) + b_n \cos(n\theta))\right)\right.$$
$$\left. + \sum_{n=1}^{\infty}(a_n' \sin(n\theta) + b_n' \cos(n\theta))\right\} \qquad (35a)$$

and

$$\sigma_y = \frac{1}{R}(G + 1) \sum_{n=1}^{\infty} n(a_n \cos(n\theta) - b_n \sin(n\theta)) \qquad (35b)$$

where the prime on the field components B, a_n, b_n denotes the derivative with respect to the radius at R. However, in the resonance condition for the spin motion, it is only the part of $\vec{\sigma}z$ which rotates with the spin that can cause significant depolarization. Hence σ must be separated into rotating and counter-rotating components. Using the relations:

$$\sin(n\theta) = \frac{1}{2i}\left(e^{in\theta} - e^{-in\theta}\right)$$
$$\cos(n\theta) = \frac{1}{2}\left(e^{in\theta} + e^{-in\theta}\right) \qquad (36)$$

σ may be analyzed into the following components:

$$\sigma = \sigma_o + \sum_{n=1}^{\infty}\left\{\sigma_{+n}e^{\imath n\theta} + \sigma_{-n}e^{-\imath n\theta}\right\} \tag{37}$$

where:

$$\sigma_o = (\gamma G + 1)\frac{B'(r)}{B(r)} \tag{38a}$$

$$\sigma_{\pm n} = \frac{1}{2}\left\{(\gamma G + 1)\left(\frac{B'}{B}b_n + b_n'\right) \mp \frac{1}{R}(G + 1)b_n n + \imath\left(\mp(\gamma G + 1)\left(\frac{B'}{B}a_n + a_n'\right) + \frac{1}{R}(G + 1)a_n n\right)\right\} \tag{38b}$$

What is of greater importance is the magnitude of these rotating components given by:

$$|\sigma_{\pm n}| = \frac{1}{2}\left\{\left[(\gamma G + 1)\left(\frac{B'}{B}b_n + b_n'\right) \mp \frac{G + 1}{R}b_n n\right]^2 + \left[\mp(\gamma G + 1)\left(\frac{B'}{B}a_n + a_n'\right) + \frac{G + 1}{R}a_n n\right]^2\right\}^{1/2} \tag{39}$$

Notice that unless the field components a_n, b_n and B are independent of radius, the magnitudes of the rotating and counter-rotating components will not be equal. Since in any isochronous cyclotron B increases with radius, and a_n and b_n have rapid radial variations at small radii where the hills of each sector begin, this inequality can be quite significant.

Recalling an equation similar to equation (23) for the vertical betatron motion, where ϕ_o is set to zero,

will complete the Fourier analysis of $\vec{\sigma}z$ giving:

$$\sigma z = z_m \cos(\nu_z \theta)\left\{\sigma_o + \sum_{n=1}^{\infty} \sigma_{+n} e^{\imath n\theta} + \sigma_{-n} e^{-\imath n\theta}\right\}$$

$$= \frac{z_m}{2}\left\{\sigma_o(\exp(\imath\nu_z\theta) + \exp(-\imath\nu_z\theta)) \right. \qquad (40)$$

$$+ \sum_{n=1}^{\infty}\left\{\sigma_{+n}(\exp(\imath(n + \nu_z)\theta) + \exp(\imath(n - \nu_z)\theta))\right.$$

$$\left.\left. + \sigma_{-n}(\exp(-\imath(n + \nu_z)\theta) + \exp(-\imath(n - \nu_z)\theta))\right\}\right\}$$

Since $\theta = \omega_c t$, the rotational frequencies present in the transverse plane are:

$$(n \pm \nu_z)\omega_c \qquad (41)$$

where $n = 0, \pm1, \pm2, \ldots$. As before, positive frequencies correspond to a rotation in the same direction as the ion's cyclotron rotation, and negative frequencies to the opposite direction. Since resonance only occurs when the precession frequency of the spin is equal to the rotational frequency of the perturbation, the resonance can occur whenever:

$$\Omega_o = \gamma G\omega_c = (n + l\nu_z)\omega_c \qquad (42)$$

or simply:

$$\gamma G = n + l\nu_z \qquad (43)$$

where $n = 0, \pm1, \pm2, \ldots$ and $l = \pm1$. Both γ and ν_z are

in general energy dependent so that the resonance condition is only encountered at specific energies during acceleration.

During the acceleration of an ion in a cyclotron, the energy increases almost linearly with time. Thus, unlike the fixed resonance condition discussed in section (5.3). it is essential to examine the effect on the ion's spin of a linear passage of an isolated resonance. Linear passage implies that the difference in the frequencies between both terms in equation (42) varies linearly with time, hence in both energy and θ. i.e.:

$$\left|\frac{d}{d\theta}\left(\omega_c\gamma G - \omega_c(n + 1\nu_z)\right)\right| = \lambda\omega_c \qquad (44)$$

where λ is a constant characterizing the rate of passage. If the energy gain per turn is ΔE then equation (44) can be written as:

$$\lambda = \left|\frac{1}{2\pi}\left\{\left(\frac{\Delta E}{E_o}\right)G \mp \Delta E \frac{d\nu_z}{dE}\right\}\right| \qquad (45)$$

where E_o is the rest mass energy of the ion.

In the case where only one resonance is crossed the spin equation of motion is:

$$\frac{d\vec{s}}{d\theta} = \vec{s} \times (\Omega(\theta)\hat{k} + \vec{\omega})/\omega_c \qquad (46)$$

where $\vec{\omega}$ is the transverse perturbation seen by the spin. It is given by:

$$\vec{\omega} = (\vec{\sigma}_n z_m \omega_c/2)(\exp(\imath(n + 1\nu_z)\theta) \qquad (47)$$

where z_m is the maximum height of the vertical betatron oscillation for the particle with spin $\vec{s}$. If Ω_o is the precession frequency at resonance, $(n + 1\nu_z)\omega_c$, then from equation (44):

$$\Omega(\theta) = \Omega_o + \omega_c \lambda \theta \qquad (48)$$

and $\vec{\omega}$ rotates in the x-y plane with frequency Ω_o. If at $\theta \to -\infty$, i.e. at $t \to -\infty$, $\vec{s} = s_z \hat{k}$, with $s_z = 1$, then equation (46) can be solved analytically for the limit of s_z as $\theta \to \infty$. (see Froissart and Stora, 1962, or Khoe et al., 1975). This limit is given by:

$$\frac{s_z(\theta \to \infty)}{s_z(\theta \to -\infty)} = 2\exp\left(-\frac{\pi}{2\lambda}\left(\frac{\omega}{\omega_c}\right)^2\right) - 1 \qquad (49)$$

Two limiting cases are of interest in equation (49). First if:

$$\frac{1}{\lambda}\left(\frac{\omega}{\omega_c}\right)^2 << 1 \quad \text{then } s_z(+\infty) \simeq s_z(-\infty) \qquad (50)$$

This corresponds to the case of "fast passage", in which the resonance condition is fulfilled for so short a period of time that no significant reorientation of the spin occurs. If the effective magnetic field description, from equation (13) and figure 11 , is used then in the "fast passage" $\vec{B}_{eff}$ goes from parallel to antiparallel

with respect to the z-axis. This reversal of $\vec{B}_{eff}$ is much faster than the spin's precession time about the transverse component of the field, so that s_z does not change significantly.

Second, if:

$$\frac{1}{\lambda}\left(\frac{\omega}{\omega_c}\right)^2 >> 1 \quad \text{then } s_z(+\infty) \simeq -s_z(-\infty) \tag{51}$$

This is "slow" or "adiabatic passage". In this case, the effective magnetic field in the rotating coordinate system changes direction so slowly that the spin essentially remains aligned with this field. As the resonance is crossed, the effective field reverses its vertical direction, causing a complete reversal of the vertical spin orientation.

5.6 Imperfections, Higher Order Effects and Corrections

The previous discussion showed how spin depolarization resonances of the form $\gamma G = n \pm \nu_z$ arise in an ideal field for a cyclotron. If n is a multiple of the N-fold symmetry of the cyclotron, i.e. a_n or b_n is non-zero in equation (20), then resonances of this form are called "intrinsic resonances" since they could not be eliminated without disturbing the ideal field. Resonances of this type are first order intrinsic resonances since only the terms to first order in z

were retained from equation (28). Other resonances are possible if the magnetic field has imperfections which cause deviations from the N-fold symmetry or transverse fields in the median plane, or if more of the higher order terms are retained in equation (28).

If the magnetic field has imperfections in the B_z field which produce deviations from the N-fold symmetry of the field, then some of the coefficients a_n and b_n and hence $\sigma_{\pm n}$ will be non-zero for n not an integral multiple of N. These coefficients can then also produce a resonance condition at:

$$\gamma G = n \pm \nu_z \quad \text{or} \quad \gamma G = -n \pm \nu_z \tag{52}$$

as in equation (42). Since $\sigma_{\pm n} \neq 0$ only if there are n^{th} order imperfections, resonances of the form in equation (52) where n is not an integral multiple of N are called imperfection resonances. The effect of such resonances can be removed by adjusting the magnetic field so that $\sigma_{\pm n} = 0$ without affecting the normal operation of the cyclotron.

Any real cyclotron's magnetic field also has some deviations from median plane symmetry arising from small mechanical asymmetries in the construction of the magnet, from some small non-uniformities in the permeability of the iron or other similar effects. It is

necessary to remove most of such defects for normal operation but there always exist some slight deviations. The effect of these imperfections may be represented by adding explicit median plane transverse fields to the expansion for B_r and B_θ, thus equation (22) would become:

$$B_x \simeq B_r = B_r(r,\theta)\Big|_{z=0} + \frac{\partial B_z}{\partial r} z + \ldots$$
$$B_y \simeq B_\theta = B_\theta(r,\theta)\Big|_{z=0} + \frac{1}{r}\frac{\partial B_z}{\partial \theta} z + \ldots \tag{53}$$

The fields $B_r(r,\theta)\Big|_{z=0}$ and $B_\theta(r,\theta)\Big|_{z=0}$ can be expanded in a Fourier series in θ, and substituted into the spin motion equation (28). A similar analysis for the resonance condition shows that resonances will occur for:

$$\gamma G = n \tag{54}$$

for $n = 0, \pm 1, \pm 2, \ldots$ These are also known as imperfection resonances.

Similarly, if the terms of higher order in z and x in the transverse field expansion are retained in the spin motion equation then other resonances are also possible. The general form of these higher order terms is:

$$U_{n,l+m}\, z^l x^m \tag{55}$$

where $U_{n,l+m}$ is related to an $l+m$ order derivative of the

n^{th} Fourier component of B_z in the median plane, and $l \geq 1$, $m \geq 0$. The resonance condition for these terms occurs at:

$$\gamma G = n \pm l\nu_z \pm m\nu_r \ , \qquad \begin{matrix} l \geq 1 \\ m \geq 0 \end{matrix} \tag{56}$$

Such a resonance is called an l+m order intrinsic resonance whenever n is a multiple of N, and an l+m order imperfection resonance otherwise. Resonances with order higher than 1 tend to be quite weak since the strength of the transverse field in equation (55) is proportional to:

$$\left(\frac{z}{r}\right)^l \left(\frac{x}{r}\right)^m \tag{57}$$

and $\frac{z}{r}$, $\frac{x}{r}$ << 1 for most particle trajectories.

Two other effects from the inclusion of higher order terms are the frequency modulation of Ω_o, the spin precession frequency, and the deviation of the EOs from being circular orbits. Since the transverse field component which rotates exactly in phase with the spin precession causes the depolarization, the Fourier expansion of σ_n should be in the spin precession angle, $\phi_p = \int \Omega dt$ where Ω is given by equation (30). The scallopping of the equilibrium orbits results in the instantaneous x and y coordinate axes being rotated slightly with respect to the r and θ coordinate system at each point on the orbit. As a particle moves around an

EO, the x-axis' direction oscillates about the radial direction and the y-axis' direction oscillates about the angular direction. These small oscillations also produce small corrections to the effective σ_n. Again, for most cyclotrons these effects can be neglected. If these higher order effects are significant, the exact integration of the coupled spin and particle motion in the accelerator will be more reliable for estimating the depolarization.

5.7 Application to the University of Manitoba Cyclotron

The severe loss of polarization when polarized H^- ions are accelerated in the U of M cyclotron may be attributed to a strong first order intrinsic resonance. The g-factor for the proton is 5.5857, and the mass ratio of the H^- ion to the proton is 1.001089, hence the effective g-factor for the H^- ion is:

$$g' = -5.5918 \tag{58}$$

and thus:

$$G = -3.7959 \tag{59}$$

The magnitude of G is sufficiently close to 4, the symmetry of the U of M cyclotron, that the first order intrinsic resonance:

$$\gamma G = -3.7958\gamma = -4 + \nu_z \tag{60}$$

can occur.

This case can be compared to the acceleration of polarized D^- ions in the U of M cyclotron. The g-factor for deuterons is only 0.8573 which gives an effective g-factor for the D^- ion of:

$$g' = -1.7147 \tag{61}$$

and thus G for the D^- ion is:

$$G = -1.8574 \tag{62}$$

The polarized D^- resonances possible of the U of M cyclotron are:

$$\gamma G = \begin{cases} -2 + \nu_z \\ -3 + \nu_z - \nu_r \\ -4 + \nu_z - 2\nu_r \end{cases} \tag{63}$$

All of these are very small since the first two are respectively first order and second order imperfection resonances, and the last is a third order intrinsic resonance.

A map of the vertical magnetic field B_z of the cyclotron was analyzed by the equilibrium cyclotron orbit code CYCLOP. In this code, the 4-fold symmetric part of the magnetic field map was used to find the equilibrium orbits, and the vertical and radial betatron oscillation

frequencies, ν_z and ν_r. ν_z and the quantity $4 + \gamma G$ are shown in figure 13 as a function of the energy of the H^- ion. The intersection of these two curves at 9.0 MeV indicates the location of the exact resonance condition.

To determine the strength of the depolarizing resonance, the magnetic field data were Fourier analyzed using the program POLICY. The Fourier coefficients for the fourth harmonic and its radial derivatives were used to calculate $|\sigma_{+4}|$ and $|\sigma_{-4}|$ from equation (39) as shown in figure 14 . Note the large difference in the magnitude at about 2 MeV. Near this energy the amplitudes of a_4 and b_4 are increasing rapidly with radius and produce a real proper rotating magnetic field. By 9.0 MeV this difference has decreased but it is still significant. Only σ_{-4} contributes to the intrinsic resonance of equation (60), giving for ω of equation (47):

$$\left|\frac{\omega}{\omega_c}\right|^2 = \frac{|\sigma_{-4}|^2 z_m^2}{4} = 9.18\, z_m^2 \qquad (64)$$

where z_m is the maximum height in meters of the particle's vertical betatron oscillation. With an energy gain per turn of 40 keV, the magnitude of λ from equation (45) is:

$$|\lambda| = 7.347 \times 10^{-5} \qquad (65)$$

Hence the polarization at an energy much greater than

Figure 13. ν_z and $4 + \gamma G$ as a function of H^- ion energy.

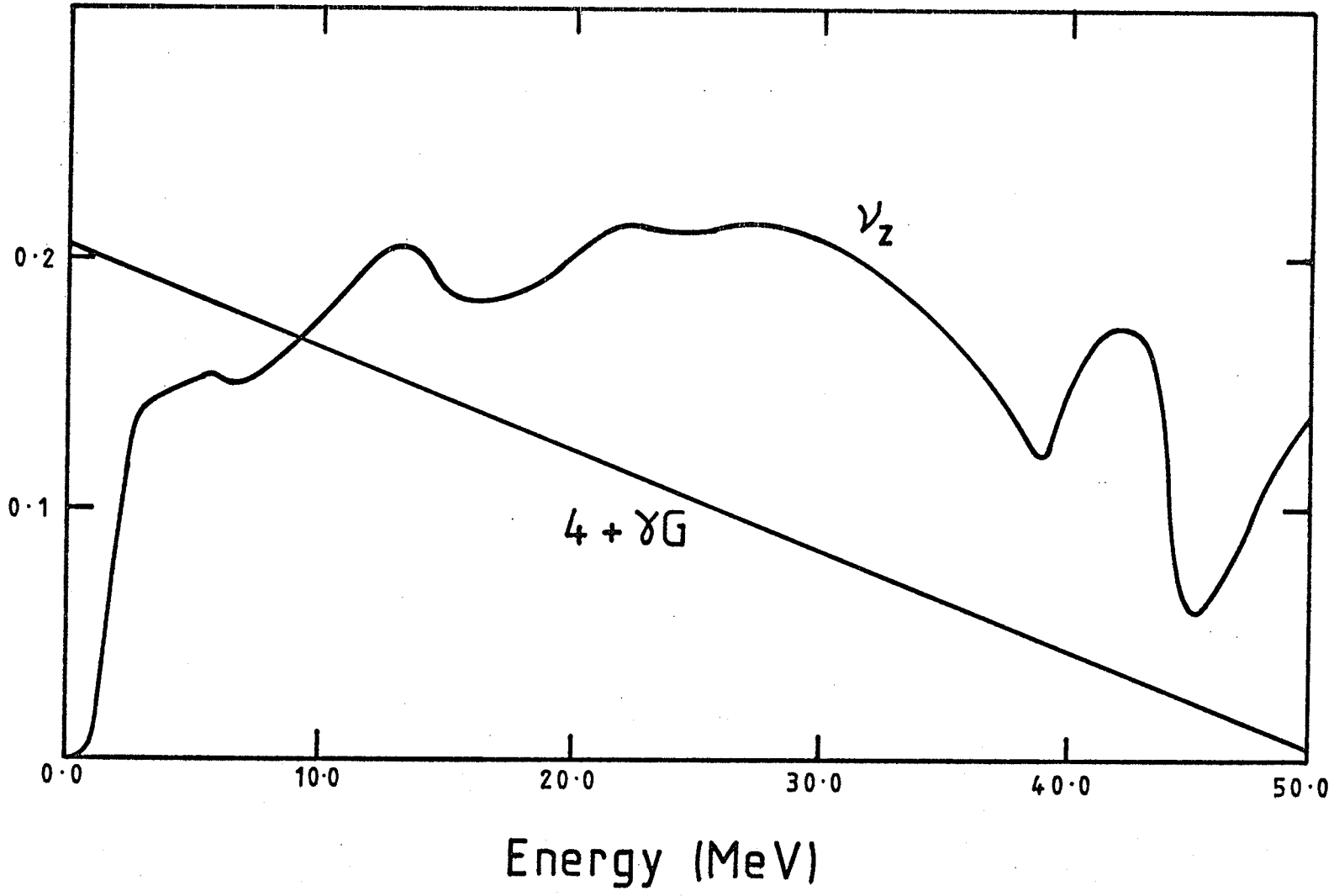
0·2
0·1
0·0
10·0
20·0
30·0
40·0
50·0
ν_z
$4 + \gamma G$
Energy (MeV)

Figure 14. $\sigma_{\pm 4}$ as a function of H^- ion energy.

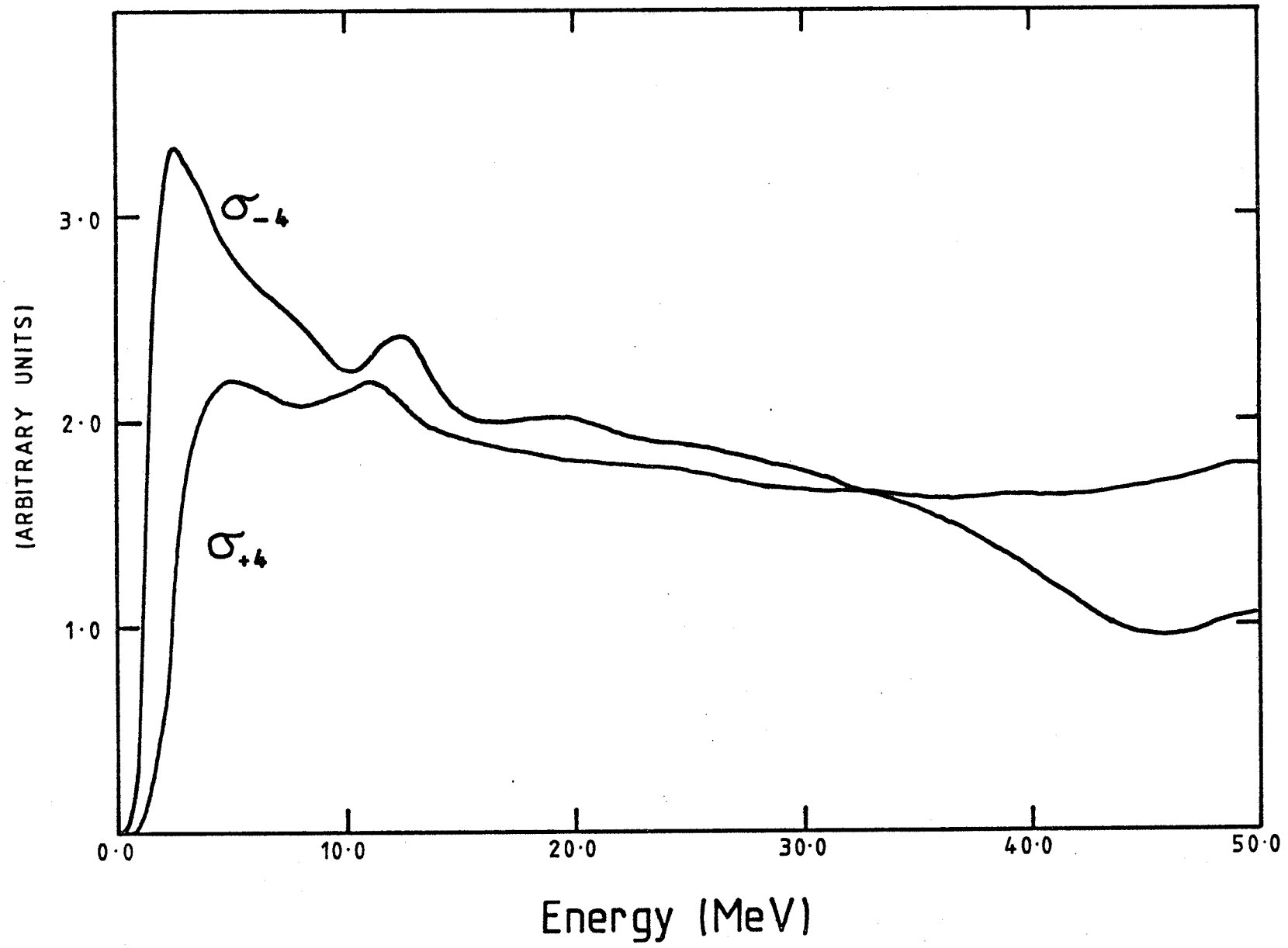
σ-4
σ+4
3·0
2·0
1·0
0·0
10·0
20·0
30·0
40·0
50·0
(ARBITRARY UNITS)
Energy (MeV)

9.0 MeV for a particle with initial $s_z = 1$ and in an orbit with maximum vertical height of z_m at resonance is:

$$s_z\Big|_{final} = 2\exp(-1.963\times10^5 z_m^2) - 1 \qquad (66)$$

This distribution is shown in figure 15 .

However, equation (66) applies only to the polarization of a single particle. To evaluate the polarization of the entire beam emerging from the cyclotron, s_z must be averaged over all phase space. Figure 16 shows the average polarization of a polarized beam after passing through the resonance as a function of the maximum beam height for a uniform distribution in the vertical beam phase space. The H^- beam at the U of M cyclotron has an estimated total vertical beam size of about 5 mm, corresponding to a maximum height from the median plane of 2.5 mm. Thus, the beam polarization for energies over 20 MeV is expected to be only 10% of the initial polarization. This is in reasonable agreement with the experimental results. The actual polarization measured will be very sensitive to changes in the vertical phase space density, which helps to explain the extreme sensitivity of the polarization to the precise operating conditions of the cyclotron.

The large loss of polarization based on these analytic estimates makes detailed calculations based upon the exact integration of the spin and particle motion

Figure 15. The final value of s_z as a function of the vertical betatron oscillation amplitude.

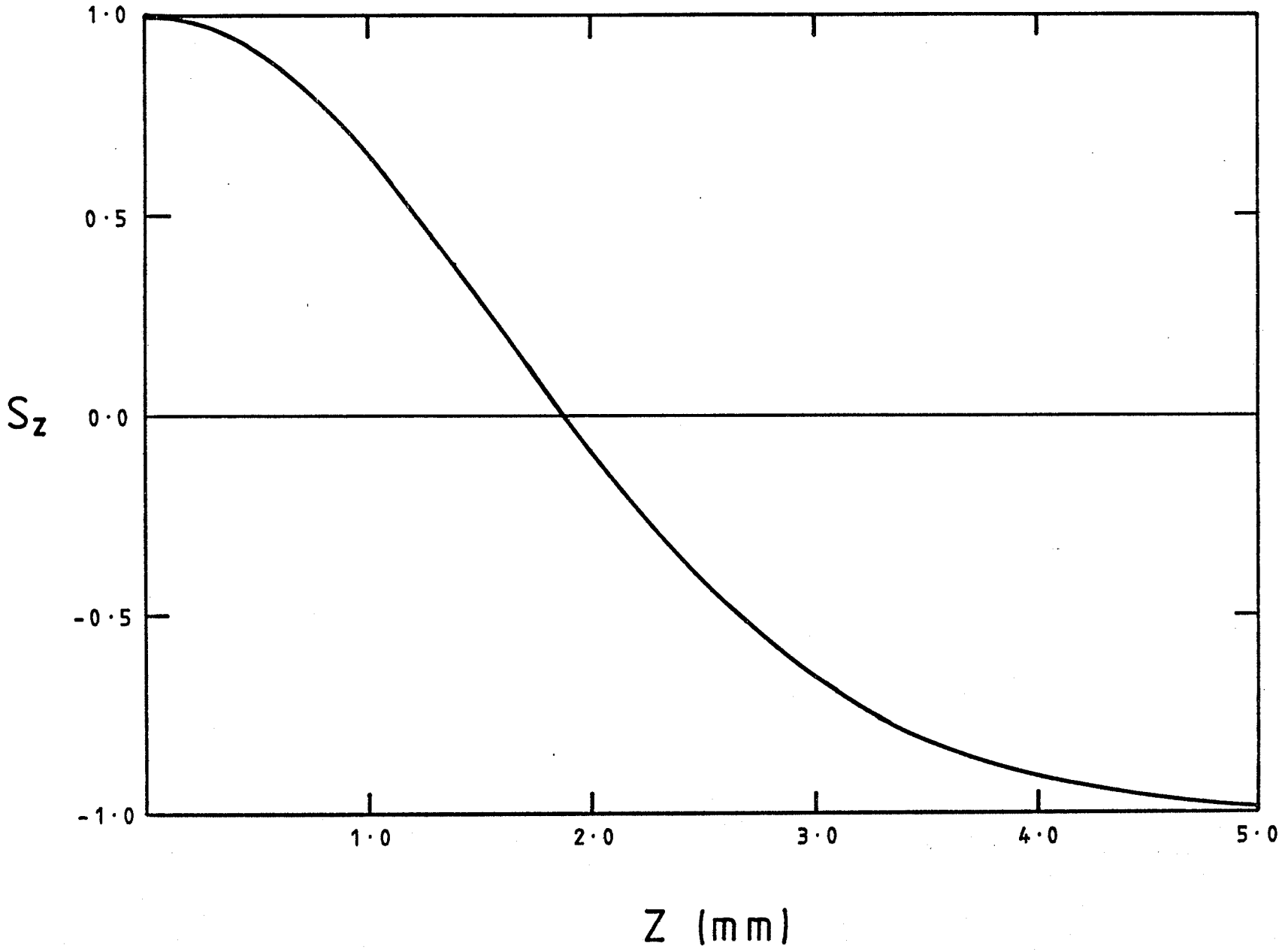
1·0
0·5
0·0
-0·5
-1·0
S_z
1·0
2·0
3·0
4·0
5·0
Z (mm)

Figure 16. The final plarization, p_z, of the accelerated H^- beam as a function of the vertical beam envelope size, assuming a uniform distribution in the vertical phase space.

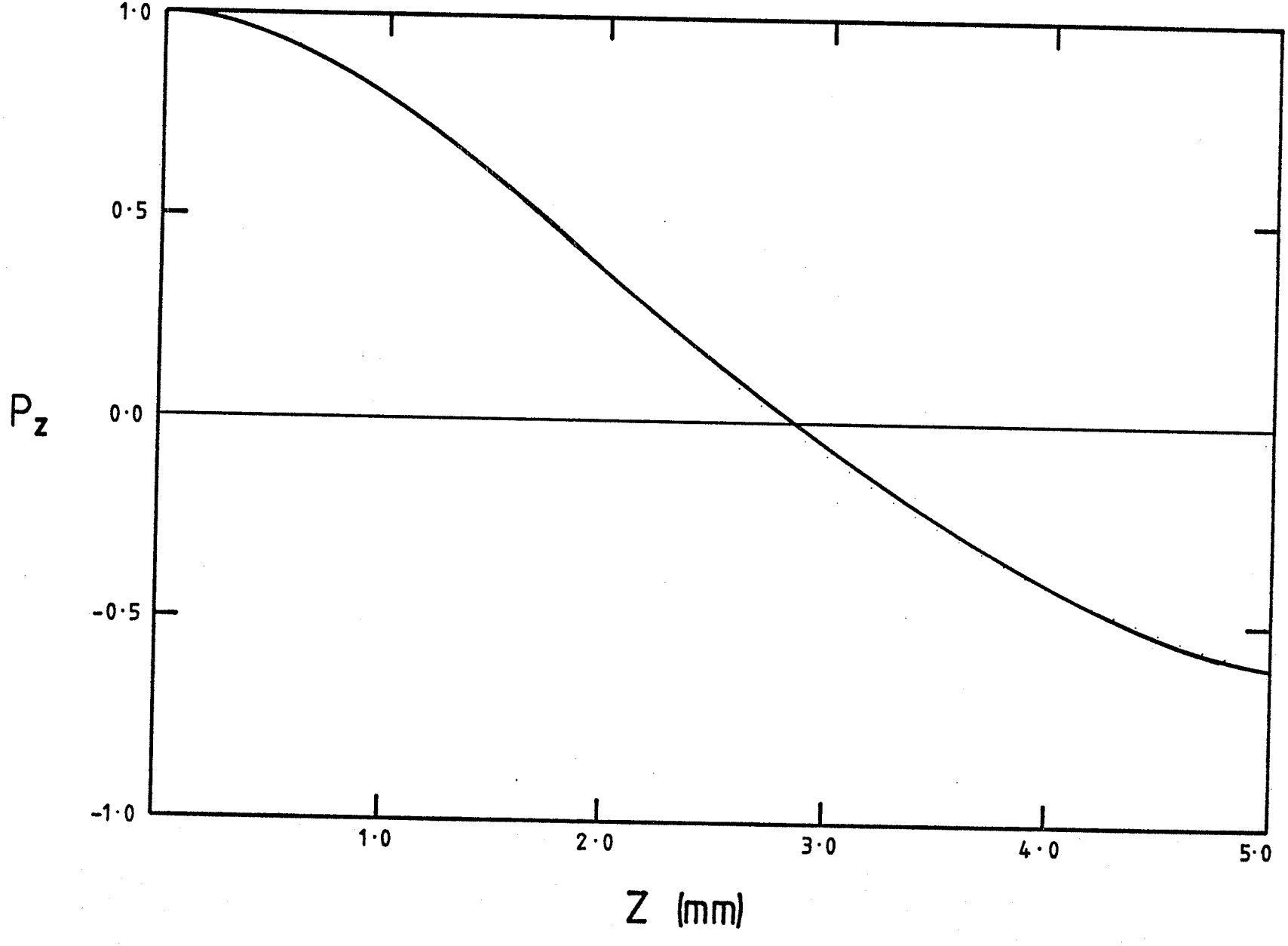
1·0
0·5
0·0
-0·5
-1·0
P_z
1·0
2·0
3·0
4·0
5·0
Z (mm)

equations essential. To perform these calculations, the general cyclotron orbit code GOBLIN was modified to describe the accelerating dees of the U of M cyclotron and to include the integration of the spin motion equation (28) for polarized H^- ions. The program GOBLIN can integrate the coupled spin and particle motion equations for one particle in the cyclotron. It includes the acceleration effects of the dees, and the magnetic field off the median plane may be treated either in the linear approximation, or in the general non-linear case. Both imperfections in the vertical field, i.e. deviations from N-fold symmetry, and transverse magnetic fields in the median plane may be included.

Some typical results for the spin motion in the U of M cyclotron are shown in figure 17 . Only the 4-fold symmetric components of the vertical magnetic field were used. These components were the same as those used in the equilibrium orbit analysis with CYCLOP. The calculation was performed with $s_z = 1$ initially, and the integration was begun at 2 MeV. S_z is plotted after each complete turn. Also shown are the analytic estimates of s_z using equation (66) and the value for z_m at 9.0 MeV as calculated by GOBLIN. Spin motion for ions less than 1 MeV in the U of M cyclotron could not be evaluated reliably with GOBLIN since the focussing effects of the electric fields at the dee gaps were not included. These

Figure 17. GOBLIN results for the motion of s_z of three particles as a function of the number of turns from 2.0 MeV. At 9.0 MeV curve 1 has z_m = 0.7 mm, curve 2 has z_m = 1.4 mm, and curve 3 has z_m = 2.1 mm. The solid lines indicate the respective analytic estimates of the final s_z determined by equation (66).

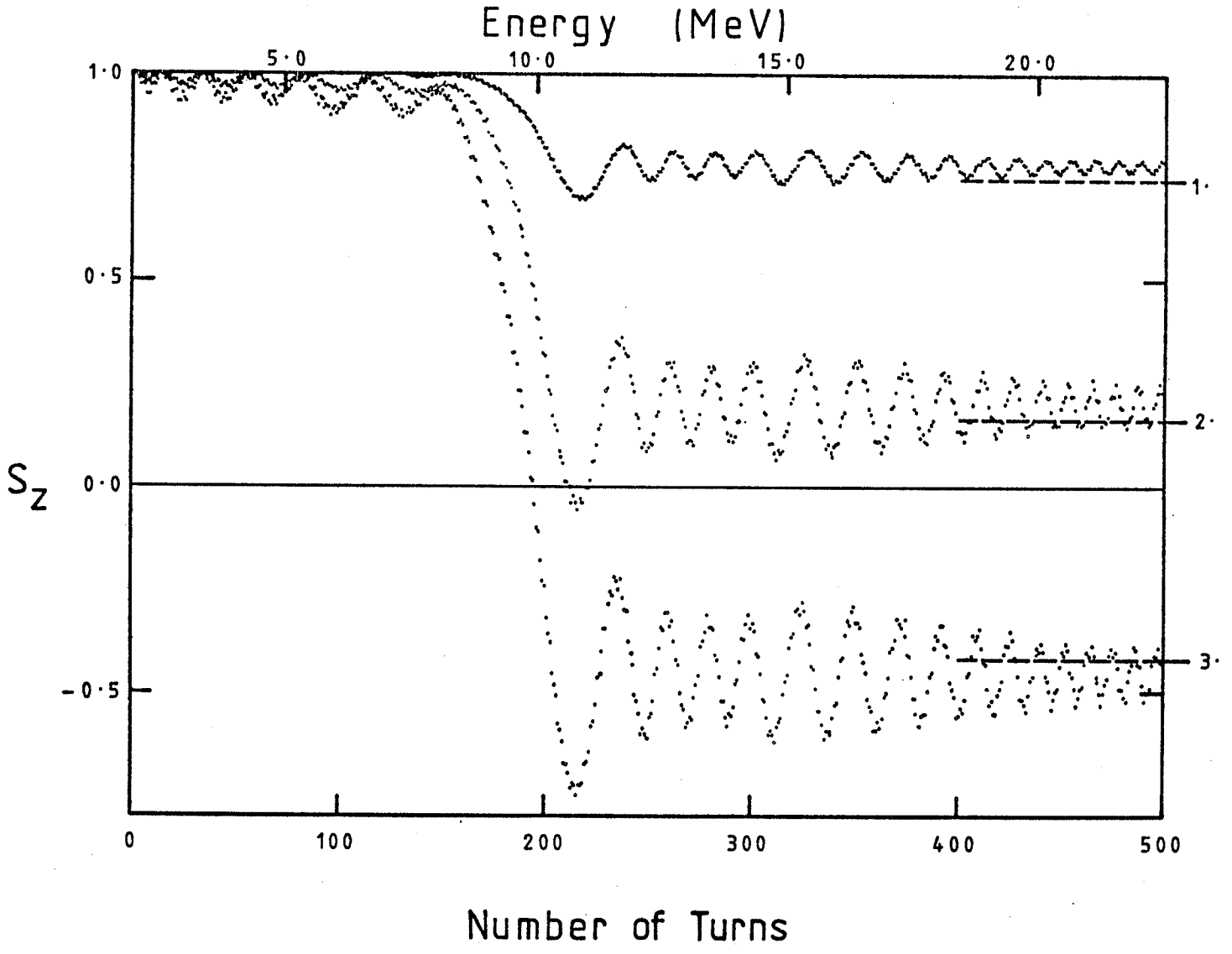
Energy (MeV)
5·0
10·0
15·0
20·0
1·0
0·5
0·0
−0·5
S_z
1·
2·
3·
0
100
200
300
400
500
Number of Turns

effects are only significant at energies less than 1 MeV.

Although the analytic formula describes the resonance crossing at 9.0 MeV well, there are some inadequacies in the case of near resonant conditions. In figure 18 , these results from GOBLIN show a second loss of polarization at 45 MeV, although the loss is less severe than that at 9.0 MeV. From figure 13 it can be seen that ν_z drops sharply towards the resonance condition, but increases again before crossing. Since there is no exact resonance, the analytic approach shows no polarization loss. Thus, even if no resonance crossing is present there can be a loss of polarization in near resonant circumstances. At present these can only be investigated by using the exact numerical integration techniques.

Figure 18. The continuation of the GOBLIN results for the motion of s_z for the same three particles as in figure 17.

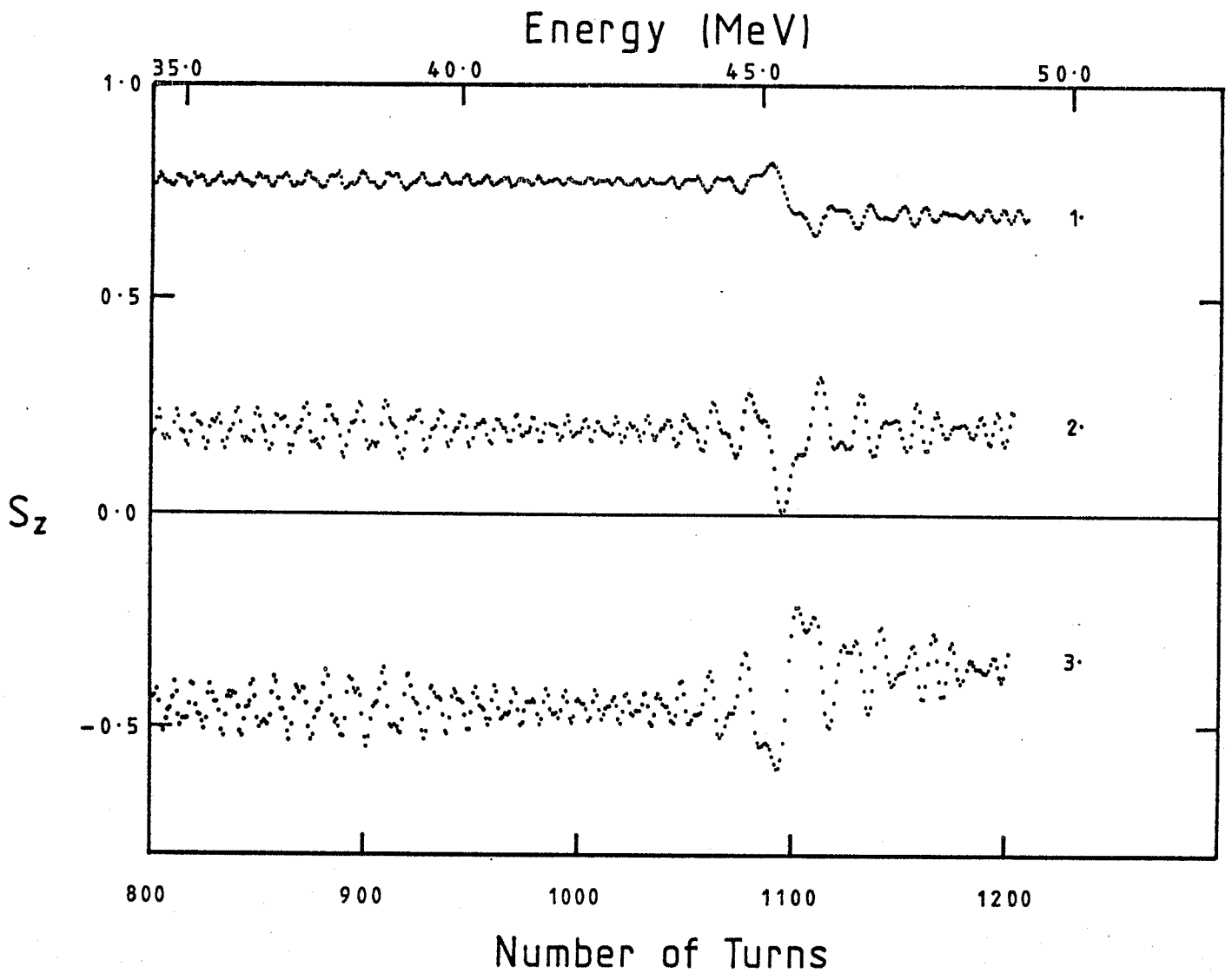
Energy (MeV)
35·0
40·0
45·0
50·0
1·0
0·5
0·0
−0·5
S_z
1·
2·
3·
800
900
1000
1100
1200
Number of Turns

CHAPTER 6

CONCLUSION

6.1 General Conclusions and Recommendations

At present the polarized ion source can deliver 100 nA of polarized H^- or D^- ions to the cyclotron for acceleration. The vector polarization p_z is between 0.75 and 0.80 for both types of ions when the quench ratio technique is used to estimate the polarization. The tensor polarization p_{zz} of the D^- ions can be changed from 0.80, with both vector and tensor polarization present, to -1.40 with pure tensor polarization. However, after acceleration through the cyclotron, only the D^- ions retain their original polarization. The H^- ions are almost completely depolarized by an intrinsic depolarizing resonance of the form:

$$-3.7956\ \gamma = -4 + \nu_z$$

This depolarization is so severe that it is recommended that development of the polarized H^- ion facility be given low priority for the near future and most development effort be placed on the polarized D^- ion capability of the U of M cyclotron.

6.2 Directions for Polarized D^- Ion Source and Cyclotron Development

The basic design of the polarized ion source appears to be sound. The operation of the source has been reliable and the 100 nA output with $p_z = 0.75$ consistently reproducible. Although this output is lower than the 300-500 nA output reported by others for this type of source, high intensity has not been emphasized during this initial development. Understanding the nature of the depolarization was of much more concern. There are several possible ways of improving the intensity:

(1) Improved alignment of the ion beams. The neutral beam in particular is 5 mm off center at the argon canal. For initial mechanical simplicity there has been no provision for adjustment of the alignment of the extractor or the other aperture lenses. Adding either a mechanical adjustment or some electric or magnetic steering elements would help considerably.

(2) Duoplasmatron and extraction optimization. The ratio of D^+ ions to the total extracted current should be improved from the present value of 60%. The extraction and accel-decel lens positions and apertures should also be optimized for maximum polarized ion output.

Several additional features should be implemented on the source to improve the convenience of operation for users. These include:

(1) The ability to adjust lens voltages and magnet currents while the source is biased at high voltage.

(2) The addition of an extra coil layer on the nuclear spin filter magnet with an independent power supply. This could be used to produce the 1 mT shifts in the nuclear spin filter magnetic field to alternate between the $m_I = \pm 1, 0$ substates.

(3) Feedback stabilization of the 1.600 GHz oscillator in the nuclear spin filter. The radio frequency electric field is quite critical in the spin filter operation and should be stabilized. At present, the unit is free running and the field strength does drift.

The overall transmission efficiency of the cyclotron is quite low when accelerating D^- ions, typically only 3%. This, and the poor quality of the extracted beam, result in the very low polarized deuteron beam currents on target. Thus emphasis should be placed on improving the D^- acceleration capability of the cyclotron.

6.3 Reducing the H^- Depolarization

For the polarized H^- beam to be useful for most nuclear physics experiments, the polarization loss should be less than 25%. In this case, beam from the ion source with a polarization $p_z = 0.80$ could be extracted from the cyclotron with $p_z \geq 0.60$. From equation (5.49) the depolarization can be reduced only by decreasing ω^2/λ. Since $\omega \propto z_m$ and this term enters equation (5.49) quadratically, the most effective way of decreasing the depolarization would be by reducing the maximum beam displacement from the median plane. However, from figure 16 , this height must be kept to less than 1.1 mm. Thus, the emittance of the beam must be kept very small, and the distortions of the orbit caused by transverse magnetic imperfections in the median plane must be removed. Such a reduction in the maximum beam height is usually not possible without a large drop in the transmission efficiency of the cyclotron. Similarly, λ could be increased, particularly by increasing the energy gain per turn. However an order of magnitude increase would be necessary and this is not possible.

Alternatively, the intrinsic resonance itself could be eliminated by more drastic changes. The symmetry of the magnetic field could be changed from a 4-sector to a 3-sector geometry. This would reduce the

amplitude of $\sigma_{\pm 4}$ to zero. Another possibility would be to accelerate polarized protons (H^+ ions). For protons, G = 1.7928 and no first order intrinsic resonances occur. Unfortunately this approach requires the cyclotron to be operated at a fixed energy and the construction of an extraction channel. Hence either reducing or eliminating the resonance will be a difficult task.

6.4 Summary

This thesis has described the construction and testing of a polarized ion source of the nuclear spin filter type which was designed for the University of Manitoba cyclotron. This is believed to be the first use of a nuclear spin filter type ion source on a cyclotron. The performance of the ion source has been reliable, but a severe depolarizing resonance was discovered during the acceleration of polarized H^- ions. Since this resonance makes the polarized H^- beam unusable for experiments a detailed analysis of its origin was made. The polarized D^- beam did not undergo any measurable depolarization, and it is the first polarized D^- ion beam to be accelerated on a cyclotron.

REFERENCES

Polarization Symposia:

1961 - Proceedings of the International Symposium on Polarization Phenomena of Nucleons (eds. P. Huber and K. P. Meyer), Helv. Phys. Acta, Supplementum VI, (Birkhäuser Verlag, Basel).

1966 - Proceedings of the Second International Symposium on Polarization Phenomena of Nucleons (eds. P Huber and H Schopper), Birkhäuser Verlag, Basel.

1971 - Polarization Phenomena in Nuclear Reactions (eds. H. H. Barschall and W. Haeberli), Univ. of Wisconsin Press, Madison.

1976 - Proceedings of the Fourth International Symposium on Polarization Phenomena in Nuclear Reactions (eds. W. Grüebler and V. Konig), Experentia Supplementum 25 (Birkhäuser Verlag, Basel).

1981 - Polarization Phenomena in Nuclear Physics - 1980 (eds. G.G. Ohlsen, Ronald E. Brown, Nelson Jarmie, W. W. McNaughton, and G. M. Hale), A.I.P. Conference Proceedings No. 69 (American Institute of Physics, New York).

Bacher, A. D., G. R. Plattner, H. E. Conzett, D. J. Clark, H. Grunder, and W. F. Tivol (1972). Polarization and Cross-section Measurements for p - ^{4}He Elastic Scattering Between 20 and 50 MeV. Phys. Rev. C5, 1147.

Bargmann, V., L. Michel, and V. L. Telegdi (1959). Precession of the Polarization of Particles Moving in a Homogenous Electromagnetic Field. Phys. Rev. Lett. 2, 435.

Batten, R. A., J. Bruckshaw, I. Gusdal, G. Knote, A. McIlwain, J. S. C. McKee, and S. Oh (1976). Axial Injection of H^- ions into the

University of Manitoba Variable Energy Cyclotron. Nucl. Instrum. Methods 136, 15.

Baumgartner, E. and H. Kim (1966). Effects of Electromagnetic Fields on Polarized Particles. UCRL - 16787, University of California, Lawrence Radiation Laboratory.

Besnier, G. (1970). Etude de la Depolarisation d'un Faisceau du Protons Accelere dans un Synchrocyclotron. Application des Calculs au S.C. du CERN. CERN 70-11. CERN, Geneva.

Bethe, H. A. and E. E. Salpeter (1957). Quantum Mechanics of One - and Two - Electron Atoms Academic Press, New York.

Birchall, J., N. T. Okumusoğlu, M. de Jong, M. S. A. L. Al-Ghazi,and J. S. C. McKee (1981). Measurement of A_y and A_{yy} in $^4He(\vec{d},d)^4He$ Scattering at 12.6 MeV. In Polarization Phenomena in Nuclear Physics - 1980 (eds. G. G. Ohlsen, Ronald E. Brown, Nelson Jarmie, W. W. McNaughton, and G. M. Hale), p. 1290. AIP Conference Proceedings No. 69.

Darden, S. E. (1971). Description of Polarization and Suggestions for Additional Conventions. In Polarization Phenomena in Nuclear Reactions (eds. H. H. Barschall and W. Haeberli), p. 39. Univ. of Wisconsin Press, Madison.

Froissart, M. and R. Stora (1960) Depolarisation d'un Faisceau de Protons Polarises dans un Synchrotron. Nucl. Instrum. Methods 7, 297.

Glavish, H. F. (1974). Polarized Ion Sources. In Proceedings of the Second Symposium on Ion Sources and Formation of Ion Beams. LBL - 3399, Lawrence Berkeley Laboratory.

Green, T. S. (1976). Beam Optics for Ion Extraction with a High-voltage-ratio Acceleration-deceleration System. J. Phys. D.: Appl. Phys., 9, 1165.

Gruebler, W., P. A. Schmelzbach, V. Konig, R. Risler, B. Jenny, and D. Boerma (1975). Investigation of Analysing Power Maxima in d - α Elastic Scattering. Nucl. Phys. A242, 285.

Hagedoorn, H. L. and N. F. Verster (1962). Orbits in an AVF Cyclotron. Nucl. Intrum. Methods 18,19, 201.

Jackson, J. D. (1975). Classical Electrodynamics 2d. ed. John Wiley, New York.

Khoe, T., R. L. Kustom, R. L. Martin, E. F. Parker, C. W. Potts, L. G. Ratner, R. E. Timm, A. D. Krisch, J. B. Roberts, and J. R. O'Fallon (1975). Acceleration of Polarized Protons to 8.5 GeV/c. Particle Accel. 6, 213.

Kim, H. G. and W. E. Burcham (1964). Resonant Depolarisation of Deuterons during Acceleration in a Sector-Focussed Cyclotron. Nucl. Instrum. Methods 27, 211.

Kirstein, P. T., G. S. Kino, and W. E. Waters (1967). Space Charge Flow McGraw-Hill, New York.

Lamb, W. E. (1952). Fine Structure of the Hydrogen Atom. III. Phys. Rev. 85, 259.

Lawrence, G. P., G. G. Ohlsen, and J. L. McKibben (1969). Source of Polarized Negative Hydrogen and Deuterium Ions. Phys. Letters 28B, 594.

Lejeune, C. (1974a). Theoretical and Experimental Study of the Duoplasmatron Ion Source. Part I: Model of the Duoplasmatron Discharge. Nucl. Instrum. Methods 116, 417.

_____ (1974b). Theoretical and Experimental Study of the Duoplasmatron Ion Source. Part II: Emissive Properties of the Source. Nucl. Instrum. Methods 116, 429.

Livingood, J. J. (1961). Principles of Cyclic Particle Accelerators. Van Nostrand, Princeton, N. J.

McIlwain, A., S. Oh, R. Abegg, R. H. Batten, J. Birchall, I. Gusdal, G. Knote, W. Mulholland, J. S. C. McKee, R. Pogson, and N. Videla (1978). Polarized Beam from the University of Manitoba Spiral Ridge Cyclotron. Nucl. Instrum. Methods 153, 283.

McKibben, J. L., R. Stevens, Jr., P. Allison, and R. A. Hardekopf (1974). Polarized H^- Source at LAMPF. In Proceedings of the Second Symposium of Ion Sources and Formation of Ion Beams.

LBL - 3399, Lawrence Berkeley Laboratory.

Ohlsen, G. G. (1970). Los Alamos Lamb-Shift Polarized Ion Source. A User's Guide. LA - 4451, Los Alamos Scientific Laboratory.

_____ and P. W. Keaton, Jr. (1973). Techniques for Measurement of Spin - 1/2 and Spin - 1 Polarization Analyzing Tensors. Nucl. Instrum. Methods 109, 41.

_____ and J. L. McKibben (1967). Theory of a Radio-frequency "Spin Filter" for a Metastable Hydrogen, Deuterium, or Tritium Atomic Beam. LA - 3725, Los Alamos Scientific Laboratory.

Pradel, P., F. Roussel, A. S. Schlachter, G. Spiess, and A. Valance (1974). Formation of H(n=2) Atoms by the Nearly Resonant Process H^+ in Cs. Multiple Collision Processes. Phys. Rev. A10, 797.

Roussel, F. P. Pradel, and G. Speiss (1977). Electron Capture, Electron Loss, and Deexcitation of Fast $H(2^2S)$ and $H(1^2S)$ Atoms in Collisions with Molecular Hydrogen and Inert Gases. Phys. Rev. A16, 1854.

Slichter, C. P. (1978). Principles of Magnetic Resonance, 2d. ed. Springer-Verlag,Berlin.

Schmelzbach, P. A., W. Grüebler, V. Konig, R. Risler, D. O. Boerma, and B. Jenny (1976). Absolute Calibration of the Analysing Powers T_{20} for the $^3He(\vec{d},p)^4He$ Reaction at 0 and iT_{11} for $^4He(\vec{d},d)^4He$ Scattering. Nucl. Phys. A264, 45.

Standing, K. G., J. J. Burgerjon, and F. Konopasek (1962). The University of Manitoba Cyclotron. Nucl. Instrum. Methods 18, 19, 111.